Shahrood University of Technology

Iranian Society of Mining Engineering (IRSME)

Journal of Mining and Environment (JME)

journal homepage: www.jme.shahroodut.ac.ir

THOMSON REUTERS

Determining Probability Distribution Functions of Rock Joint Geometric Properties

Jamal Zadhesh and Abbas Majdi*

School of Mining Engineering, College of Engineering, University of Tehran, Iran.

Article Info

Received 4 March 2022

Received in Revised form 24 March 2022

Accepted 11 April 2022

Published online 11 April 2022

DOI:10.22044/jme.2022.11724.2165

Keywords

Rock Joint Geometry Properties

Spacing, Aperture

Trace Length

Goodness-Of-Fit Tests

Abstract

The mechanisms of deformation and failure of the structures in and on the jointed rock masses are often governed by the characteristics of the geometrical properties of joints. Since the joint geometry properties have a range of values, it is helpful to understand the distribution of these values in order to predict how the extreme values may be compared with the values obtained from a small sample. This work studies three datasets of joint systems (1652 joint data) from nine outcrops of igneous, sedimentary, and metamorphic rocks in order to determine the probability distribution function of the rock joint geometry properties. Consequently, the goodness-of-fit (GOF) tests are applied to obtain the data. According to these GOF tests, the Lognormal is the best probability distribution function representing the joint spacing, aperture, and trace length. The Cauchy is the best probability distribution function for the joint dip angle. It is found that the Cauchy distribution function is the best probability distribution function to represent the joint dip direction of igneous rocks, and the Burr distribution function is the best probability distribution function to define the joint dip direction of the sedimentary and metamorphic rocks.

1. Introduction

The engineering properties of rock masses are controlled by the characteristics of the discontinuities and intact rocks [1]. In order to predict the behavior of the structures in and on such jointed rock masses, it is necessary to characterize the geomechanical properties of the joints and intact rocks. A joint is defined as a fracture in the mesoscale dimension for which no shear offset or dilation is detectable in the field [1, 2], which are found in all the component rocks within about 1 km of the Earth's surface, at all orientations and sizes ranging from a few millimeters to several hundred meters [3]. Conclusively, we apply "joints" as a field term to the mesoscale fractures that either show tensile opening, and tensile surface features (e.g., plumes) or do not have any evidence for the shear/normal displacements observable in a single continuous exposure. The joint systems in rock masses are geometrically complex. The effect of joint geometry properties to control the fluid-mechanical behavior and stability of the constructed structures in and on jointed rock masses has been extensively reported in the literature [4-27]. Therefore, the joint geometry properties must be measured precisely.

In rock engineering, determining the geo-mechanical properties of jointed rock masses is crucial, which restricts the project design, construction, and operation decisions. However, the statistical simulation is even more powerful. As a result, the probabilistic simulation helps the engineers develop more robust and economic designs and solutions [28]. Thus, the properties of joints typically vary over a wide range, and their nature of random characteristics is required to be appropriately described in the preliminary design investigations [29]. Since the natural phenomena occur with such variation, a definition of stochastic rather than a deterministic system is more realistic [30]. However, it is possible to consider the full

Corresponding author: amajdi@ut.ac.ir (A. Majdi).

range of data concerning the specific random characteristic in a stochastic estimation. This can be easily achieved with probability distributions that give both the range of values that the variable could take and the relative frequency of each value within the range [31]. Consequently, the joint geometry property distributions are directly obtained from the sample histogram of the received data from joint surveys. This work intends to determine the distribution function of the joint geometry properties.

2. A Review of Research on Geometric Properties of Rock Joints

The rock joints most commonly measuring the geometric properties are spacing (or density), trace length, aperture, and orientation. Based on the results obtained by many researchers, the statistical distributions of the joint properties are described in the following.

2.1. Joint spacing

Joint spacing is a measure of jointing intensity in a rock mass, i.e., the number of joints per unit distance normal to the orientation of the set. It is taken as the perpendicular distance between the adjacent joints [32]. This paper used the intersection length (length along the scanline to the intersection point with the joint) to describe the joint spacing. Although the mean discontinuity spacing provides a direct measure of the rock quality, several researchers have found it instructive to investigate the distribution of discontinuity spacing by plotting the histograms of the sampled values of the total spacing. The joint spacing often follows an exponential distribution based on the field measurements and the distribution of the maximum discontinuity spacing for various igneous, sedimentary, and metamorphic rocks [33, 45]. Also, the field surveys using window and scanline sampling have reported that joint spacing follows lognormal distributions [32, 38, 40, 45, 46], even though Gama distributions and bimodal distributions have also been reported [39, 45, 47].

2.2. Joint aperture

The mechanical aperture or opening of a discontinuity is the distance between the opposing interfaces measured along the mean normal to the discontinuity surface [3, 48]. Also the apertures of natural discontinuities are likely to vary widely over the extent of the joint [49]. Once the gap has been created, it can be increased naturally by the physical and chemical erosion processes induced by the flow of water along the fracture. In certain circumstances, the development of local tensile stresses in a rock mass can lead to a dramatic opening of fracture apertures to values exceeding 1 m in some cases, although the opening of fractures in this way is usually limited to the zone of de-stressed rock immediately adjacent to a free surface. It can occur at depth due to the stresses induced during hydraulic fracturing. Discontinuity apertures in the stone immediately adjacent to a free surface are also particularly susceptible to opening due to blast-induced vibrations, erosion, and the washing out of infill [3]. A research work shows that aperture depends on the stress history, normal displacement, shear displacement, and study scale [50].

The above observations suggest that the physical measurement of the discontinuity apertures at exposed rock faces can provide, at best, only a general guide to the mechanical apertures within the rock mass [3]. Numerous studies at various problem scales and in different geological settings have shown that a widescale over-scale a wide range since the variation in apertures can result from the mechanical misfits of fracture walls and chemical change action dissolution, mineral filling, and normal stresses. Fracture apertures are measured by various methods including direct measurements in cores or outcrops and deduction from flow data, and therefore, show wide scatters.

Power law distribution function of apertures has been used in some applications [12, 47, 51, 52], as confirmed by field measurements using the techniques such as micro-scanner logs, borehole televiewer, and direct measuring of outcrops [53 - 58]. In the literature, the fracture transmissivity, which is related to the hydraulic aperture through the cubic law, is usually found to follow either lognormal or power-law distributions [59, 66], even though normal distributions [40, 48, 65, 67, 50] and bimodal distributions [68] have also been reported. It is now generally recognized that the resolution and finite-size effects on a power-law population can also result in distributions that appear to be exponential or lognormal. It has been reported that mapping the resolution effects (known as truncation) imposed on a power-law population can result in a lognormal distribution since the aperture fractures with aperture values smaller than the distribution mode are incompletely sampled [69, 73]. Therefore, some researchers have assumed that aperture distribution in the fractured rocks follows a lognormal distribution, as reported in the literature [16, 59, 52, 63, 64, 66, 74]. Even though the previous researchers have conducted aperture measurement and its distribution analysis, the researchers have not introduced a clear distribution function. This study aims to determine, visualize, and interpret aperture distribution under different sites of various rock types.

2.3. Joint orientation

Joint orientation describes the attitude of the joint in space. The plane of a joint in space is defined by the dip of the line of steepest declination measured from horizontal and by the dip direction measured clockwise from true north. In the outset research, it has been found that the joint orientation follows a normal distribution [32, 75]. However, the literature has recently reported that joint orientation distribution in fractured rock masses follows a Fisher distribution [16].

2.4. Joint trace length

As observed in an exposure, joint length is a distance from the intersection point on the scanline to the end of the joint trace. There will be two semi-trace lengths associated with each discontinuity: one to the left and one to the right of a scanline along the maximum dip line of the face. It can be helpful to keep a record of the nature of the termination of each semi-trace. 1: The discontinuity trace terminates in the intact rock material, 2: termination at another discontinuity, 3: termination is obscured. A trace can be obscured by block rocks, scree, soil, vegetation or extend beyond the exposure limits [3]. Several biases exist in the sampling trace lengths and inferring joint size. These have been discussed in [42, 76], and will not be repeated here. The question of censoring involves the joint traces that are not entirely observable. The most common reason a joint trace is not wholly observable is that it runs off the outcrop or into a wall (Figure 1). Thus one knows only that the actual trace length is longer than observed for that observation. Since more extended traces are more likely to be censored than the shorter ones, these incomplete observations cannot be ignored [33].

The stated distributions of joint trace length are less reliable than those for other geometrical properties, perhaps partly due to solid biases implicit in many standard sampling plans and partly due to the way the data is grouped into histograms before analysis, although the physical processes that control the other joint properties are relatively easy to understand compared to the physical mechanisms that control the joint length. In theory, the differences in the observed distribution of joint sizes result from differences in the mechanical processes creating the joints; for example, [73] argues that a uniform stress distribution would lead to exponential distributions, while the multiplicity processes such as breakage may lead to a lognormal distribution. Perhaps the most frequently reported distribution functions are lognormal and exponential.

The joint trace length is often found to follow a lognormal distribution [17, 18, 32–36, 42–46, 73-81]. Also field surveys using the techniques such as window and scanline sampling have reported that joint trace length follows exponential distributions [33, 36, 40, 45, 82, 83, 84] and power-law distribution [16, 59-66]. However, some investigations have reported Gama distributions [39, 45].

Trace length indicates the size joint plane. It can be approximately measured by detecting the joint trace lengths on the surface exposures [85]. Often rock exposures are small compared to the area or length of joints, and the actual length can only be guessed. This study introduces a new technique for joint trace length estimation. The new approach uses the support vector machine (SVM). SVM is an excellent kernel-based tool for binary data classification and regression [86-89]. This learning strategy introduced by [90] is a moral and compelling method in machine learning algorithms. It may be possible to record other geometrical properties of exposed joints accurately, and, at this moment, a trained SVM model can estimate the trace length. We prepared three datasets that included 1652 joints from the igneous, sedimentary, and metamorphic rocks in order to achieve the purpose of this study. The joint properties such as intersection distance of the joint on the scanline, aperture, orientation (dip and dip direction), roughness, Schmidt rebound of the joint's wall, and sets a number of the joint that could be measured accurately, and the surveyed location of the exposure were used as an input para, and joint trace length predicted as an output meter parameter. The datasets were randomly divided into the training and testing datasets. In each model, 70% of datasets were considered for training, and the rest was kept for testing the models. Finally, obscured prepared was for each rock type predicted joint trace length. The details of this method to estimate the joint trace length are explained by [77].

3. Description of data collection

The geometric properties of jointing are inferred primarily from the observations in outcrops and openings. While advances in the statistical techniques for inferring fracture patterns from drill cores are made, these are yet found application from a practical viewpoint. The observations made in the outcrop are joint traces, i.e. of the intersections of joint planes with the outcrop [91].

Joint surveys are an essential section of site description studies in rock engineering. The strength, deformation, and flow behavior of jointed rock masses are strongly influenced by rock mass joints' geometry and engineering properties [33]. Measuring the joint geometry parameters is commonly determined by conducting surveys along the exposed rock faces using line-sampling or window-sampling techniques [83]. Both methods have the disadvantage of mapping only exposed surfaces. Thus they cannot determine the structural behavior behind the exposed surface. In scanline mapping, less judgment is required during the actual data collection; hence not much geological mapping experience is required. Although more data is collected over larger areas in window mapping, the data from scanline mapping represents more detailed information per specific location [78]. The collected data reported in this paper was obtained from the scanline mapping technique only. The scanline mapping technique has been described in more detail by [92]. It involves a relatively simple, reproducible, and systematic method for discontinuity mapping on more prominent exposed rock faces (e.g. quarry or road cuts). The technique enables the orientation data, joint frequency, spacing, trace length, and fracture termination estimates to be made and treated statistically [93]. A measuring tape is usually used as a scanline, and the properties of only those joints that cross the tape are recorded. Figure 1 shows the scanline sampling and the type of joint terminations. The qualities and quantities of the measured data of geometric properties obtained from field mapping on outcrops of limited areas and borehole logging of narrow borehole diameters and depths contain significant uncertainty.

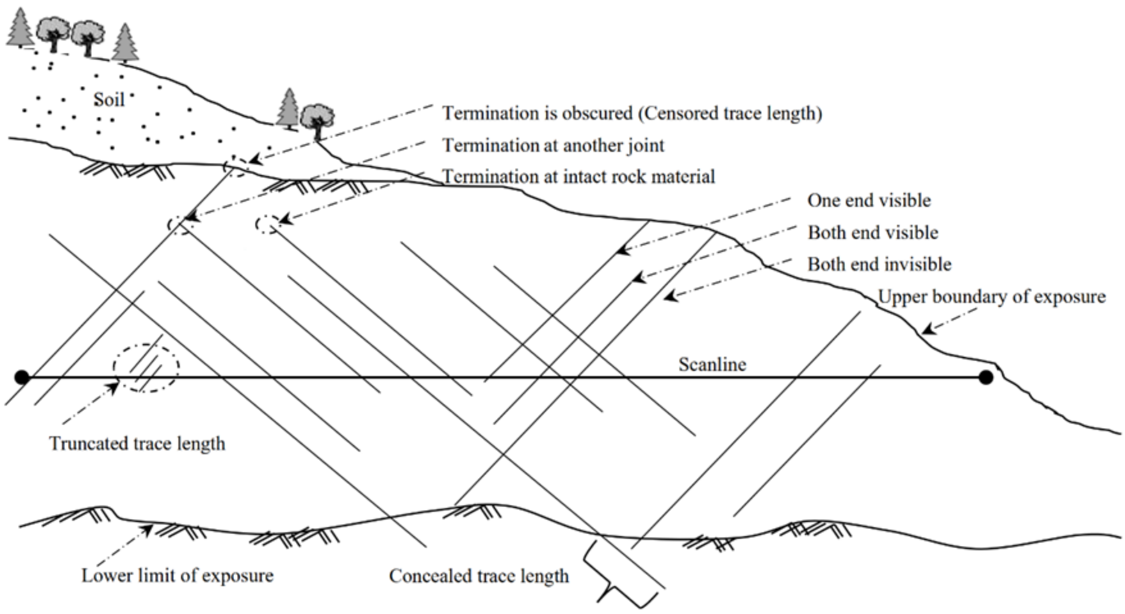

Figure 1. Scanline sampling and description of joint terminations [77].

In order to obtain a fracture system more realistically, a clean, approximately planar rock face is selected that is large relative to the size and spacing discontinuities exposed [3]. Also the sample zone should contain 150 to 350 joints, about 50% of which should have at least one end visible. Thus the outcrops of Sarshiw andesites located 40 km from the Marivan city in the Kurdistan province, west of Iran for igneous and metamorphic rocks, and Tazare coal mine located 70 km from Shahrood city, Semnan province, north-east of Iran for sedimentary rocks were selected for the research work, although the most existing joints in the selected outcrops have one end visible. Figure 2 shows a three-view of selected outcrops of all surveyed rock types. In addition, the summary of the conducted joint surveys and statistical overview of the joint geometry properties are shown in Table 1 and Table 2, respectively.

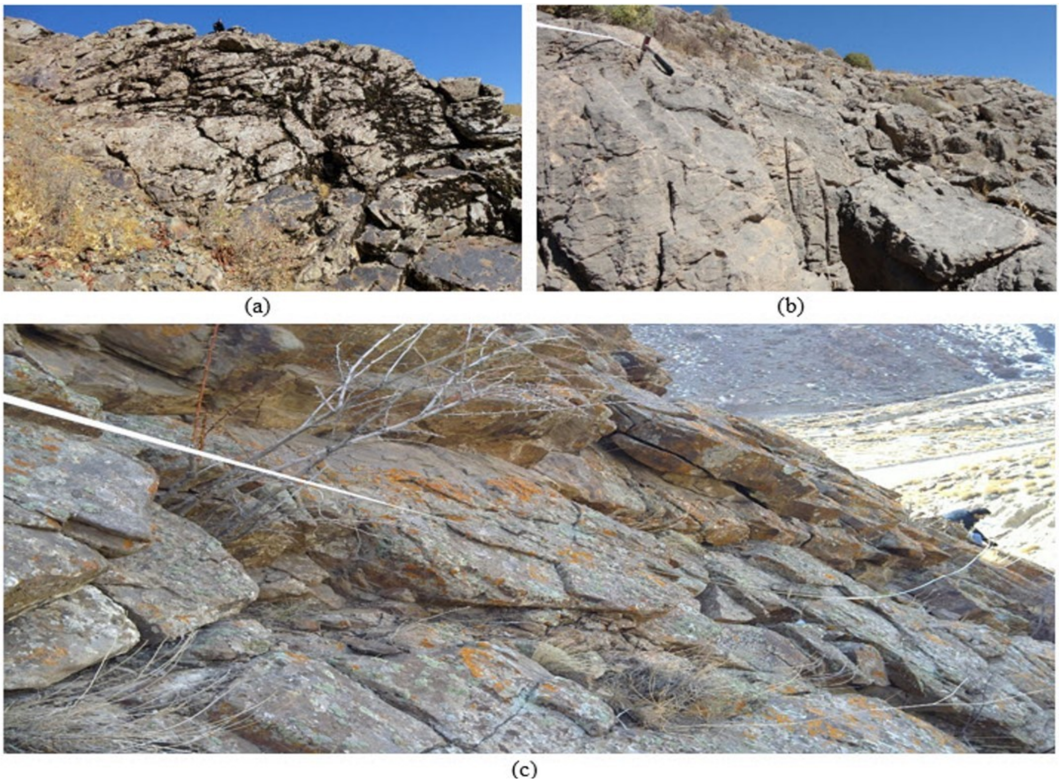

Figure 2. Views of rock exposures: (a) Sarshiw andesite, (b) Sarshiw metamorphic, and (c) Sedimentary rock of Tazare coal mine.

The inability to discriminate the joints smaller than the detection limits of the measurement is a form of sampling bias known as truncation. The upper bound of the joint trace length distribution is affected by the exposure conditions. This phenomenon represents another sampling bias called censoring [69, 73]. In order to have a view of the type of the joint trace length termination in the outcrop, suppose the numbers to three types of traces be p, m, and n for joints with both of the traces censored, one end of trace censored, and both ends of the trace observable, respectively (all types are shown in Figure 1) [39]. Then R_0, R_1, and R_2 are defined as Equations 1a, 1b, and 1c.

$$\begin{cases} R_0 = p/(p+m+n) & (1a) \\ R_1 = m/(p+m+n) & (1b) \\ R_2 = n/(p+m+n) & (1c) \end{cases}$$

For all joints of three rock types, R_0, R_1, and R_2 were calculated and shown in Table 1.

Table 1. Summary of conducted joint surveys.

Rock type	Site	Number of joints	Number of joint sets	Type of termination		
				R_0	R_1	R_2
Igneous	SI1	195	5	0.12	0.21	0.67
	SI2	201	4	0.20	0.23	0.57
	SI3	160	3	0.13	0.18	0.69
Metamorphic	SM1	165	3	0.40	0.17	0.43
	SM2	210	3	0.37	0.21	0.42
	SM3	143	4	0.34	0.10	0.56
Sedimentary	SS1	173	4	0.27	0.17	0.56
	SS2	224	3	0.23	0.25	0.52
	SS3	181	4	0.19	0.19	0.62

Table 2. Statistical summary of joint geometry properties.

Site	joint geometry properties													
	Spacing (m)		Aperture (mm)		Orientation				Trace length (m)				SRH***	
					Dip (degree)		Dip direction (degree)		Obs.*		SVM**			
	Ave.	St. dev	Ave.	St. dev	Ave.	St. dev	Ave.	St. dev	Ave.	St. dev	Ave.	St. dev	Ave.	St. dev
SI1	0.79	0.83	6.43	9.52	66	23.0	194	100.0	2.59	1.65	3.82	3.91	60	11.0
SI2	0.74	0.97	3.99	6.11	65	24.5	181	93.44	2.24	1.88	3.28	4.56	66	8.11
SI3	1.41	1.09	124.3	153.1	69	16.1	179	83.10	5.15	6.90	5.58	6.90	50	7.50
SM1	1.61	1.26	173.9	156.7	73	8.80	155	76.40	7.59	7.40	8.02	7.50	35	6.00
SM2	1.19	1.34	183.8	326.6	66	18.5	108	47.90	5.09	8.20	7.15	13.3	42	10.6
SM3	1.21	0.95	50.4	48.36	63	11.60	128	69.29	2.96	4.04	3.08	4.14	39	8.23
SS1	0.48	0.33	22.8	20.37	70	14.40	136	79.65	3.37	2.62	3.63	3.03	30	6.40
SS2	0.27	0.26	5.2	8.91	77	9.64	235	101.84	1.13	1.00	2.21	4.40	28	9.20
SS3	0.32	0.29	14.21	11.25	72	15.20	141	81.43	2.45	2.11	3.51	5.15	31	8.15

*Observation trace length

**Estimation trace length using SVM models (This method will be explained later.)

***Schmidt Hammer Rebound

4. Goodness-of-Fit (GOF) Tests

The GoF tests measure the compatibility of a random sample with a theoretical probability distribution function. In other words, these tests show how well the selected distribution fits the measured data. In this work, three GoF tests, namely Kolmogorov-Smirnov test, Anderson-Darling test, and Chi-Squared test, were used to evaluate the probability distribution of the rock joint geometry properties data obtained in nine outcrops of three rock type surveys.

The **Kolmogorov-Smirnov** test is used to decide if a sample comes from a hypothesized continuous distribution. It is based on the Empirical Cumulative Distribution Function (ECDF). Assume a random sample x_1, ..., x_n from some distribution with CDF F(x). The empirical CDF is denoted by Equation 1.

$$F_n(x) = \frac{1}{n}.\left[Number\ of\ observation \le x\right] \tag{2}$$

The Kolmogorov-Smirnov statistic (D) is based on the largest vertical difference between the theoretical and empirical cumulative distribution function, as shown in Equation 2.

$$D = \max_{1 \le i \le n}\left(F(x_i) - \frac{i-1}{n}, \frac{i}{n} - F(x_i)\right) \tag{3}$$

The **Anderson-Darling** procedure is a general test for comparing the fit of an observed cumulative distribution function with an expected cumulative distribution function. This test gives more weight to the tails than the Kolmogorov-Smirnov test. The Anderson-Darling statistic (A^2) is defined as Equation 3.

$$A^2 = -n - \frac{1}{n}\sum_{i=n}^{n}(2i-1).\left[\ln F(x_i) + \ln(1 - F(x_{n-i+1}))\right] \tag{4}$$

The **Chi-Squared test** is used to determine if a sample comes from a population with a specific distribution. This test is applied to the binned data, so the value of the test statistic depends on how the data is binned. The Chi-Squared statistic is defined as Equation 4.

$$x^2 = \sum_{i=1}^{k}\frac{(O_i - E_i)^2}{E_i}, \tag{5}$$

where O_i is the observed frequency for bin I, and E_i is the expected frequency calculated by Equation 5.

$$E_i = F(x_2) - F(x_1), \tag{6}$$

where F(x) is the CDF of the probability distribution being tested, and x_1 and x_2 are the limits for bin I [94].

The hypothesis regarding the distributional form is rejected at the chosen significance level (α) if the tests statistic, D, A^2, and x^2 for Kolmogorov-Smirnov test, Anderson-Darling test, and Chi-Squared test, is greater than their obtained critical value. The fixed values of α (0.01, 0.05, etc.) are generally used to evaluate the null hypothesis (H_0) at various significant levels. A value of 0.05 is typically used for most applications. Therefore, the 0.05 value was used in this work.

The GoF tests statistics of the Kolmogorov-Smirnov, Anderson-Darling, and Chi-Squared tests of related probability distribution functions of each joint geometry properties will be calculated. If each value is smaller than its critical value, it is the best probability distribution function to represent that joint geometry properties distribution function. However, in order to recognize the influences of each one of these three GoF tests together well, it is essential to normalize the difference values of critical and statistic values of each test within the range [0 1]. This normalization was performed using Equation 7.

$$Normalized\ value = \frac{X_{critical} - X_{statistic}}{X_{critical}} \quad (7)$$

$X_{Criticaland}$ and Xstatistic are critical, and the obtained statistics values. In order to minimize the weaknesses and amplify the strength of these three methods, we summed the results together. Then three normalized values of the three GoF tests for each distribution function are calculated. Consequently, the distribution function with a greater value is the best probability distribution function for representing the joint geometry properties.

5. Distribution function of rock joint geometry properties

Since this work deals with the collection and use of the joint geometrical properties, it is appropriate to graphically show some of the terms relevant to this topic. In this research work, due to the published reports of the previous researchers, the GoF test statistics were calculated for the normal, lognormal, gamma, exponential, power function, and Weibull distribution functions separately. Eventually, the best probability distribution function to represent the joint geometry properties is determined from the functional form's best fit to collect the field data.

5.1. Joint spacing distribution function

The calculated GoF test statistics of Kolmogorov-Smirnov, Anderson-Darling, and Chi-Squared tests of spacing are shown in Table 3. Also the comparison views of the summed up normalized GoF test statistics values for joint spacing of all surveyed exposures are shown in Figure 3. According to the calculated GoF test statistics, the lognormal distribution was found to be the best probability distribution function for representing a joint spacing distribution; the probability density function for a lognormal distribution is defined as Equation 8:

$$f(x) = \frac{1}{x\sigma\sqrt{2\pi}} \exp\left[-\frac{1}{2}\left(\frac{\ln x - \mu}{\sigma} \right)^2 \right] \quad (8)$$

In addition, Figure 4 to Figure 6 show three samples of the obtained lognormal distribution of joint spacing data.

Table 2. Test statistic of Kolmogorov-Smirnov, Anderson-Darling, and Chi-Squared tests of spacing.

Site	Test statistic																												The best probability distribution function
	Lognormal							Exponential							Gamma							Power Function							
	D	D_c	A^2	A^2_c	x^2	x^2_c	S	D	D_c	A^2	A^2_c	x^2	x^2_c	S	D	D_c	A^2	A^2_c	x^2	x^2_c	S	D	D_c	A^2	A^2_c	x^2	x^2_c	S	
SI1	0.14	0.24	0.87	2.50	1.33	7.82	**1.90**	0.21	0.24	0.14	2.50	3.94	7.81	1.56	0.26	0.30	1.75	2.50	2.06	3.84	0.90	0.23	0.17	5.06	2.50	11.1	7.81	-1.8	Lognormal
SI2	0.08	0.17	0.40	2.50	7.49	12.3	**1.77**	0.14	0.17	1.72	2.50	8.36	11.1	0.73	0.13	0.17	1.41	2.50	5.81	12.6	1.21	0.24	0.17	9.02	2.50	NA	NA	NA	Lognormal
SI3	0.06	0.24	0.15	2.50	0.55	7.81	**2.62**	0.16	0.24	0.72	2.50	0.84	7.81	1.94	0.08	0.24	0.42	2.50	0.17	5.99	2.47	0.30	0.24	2.83	2.50	3.34	5.99	0.06	Lognormal
SM1	0.14	0.24	0.48	2.50	2.48	7.81	1.91	0.18	0.24	0.80	2.50	0.43	5.99	1.86	0.11	0.24	0.31	2.50	3.01	7.81	**2.03**	0.21	0.24	1.84	2.50	11.2	7.81	-0.0	Gamma
SM2	0.12	0.30	0.25	2.50	0.33	3.84	**2.41**	0.18	0.30	0.46	2.50	0.94	5.99	2.06	0.18	0.30	0.58	2.50	2.68	3.84	1.47	0.37	0.30	6.08	2.50	NA	NA	NA	Lognormal
SM3	0.18	0.32	2.24	2.50	0.67	3.84	**1.37**	0.18	0.32	2.70	2.50	0.76	3.84	1.16	0.17	0.32	2.13	2.50	5.02	5.99	0.78	0.41	0.32	4.45	2.50	6.63	3.84	-1.8	Lognormal
SS1	0.09	0.20	0.45	2.50	1.36	11.1	**2.25**	0.18	0.20	2.80	2.50	8.99	7.81	-0.2	0.09	0.20	0.23	2.50	2.54	11.1	2.23	0.40	0.20	16.7	2.50	NA	NA	NA	Lognormal
SS2	0.06	0.17	0.18	2.50	0.75	11.1	**2.51**	0.18	0.17	0.86	2.50	5.53	11.1	1.10	0.08	0.17	0.69	2.50	3.12	11.1	1.97	0.22	0.17	8.34	2.50	NA	NA	NA	Lognormal
SS3	0.06	0.20	0.15	2.50	1.03	11.1	**2.54**	0.18	0.24	0.87	2.50	1.33	7.82	1.90	0.11	0.17	0.65	2.50	4.70	11.1	1.68	0.35	0.27	2.95	2.50	5.51	3.84	-0.9	Lognormal

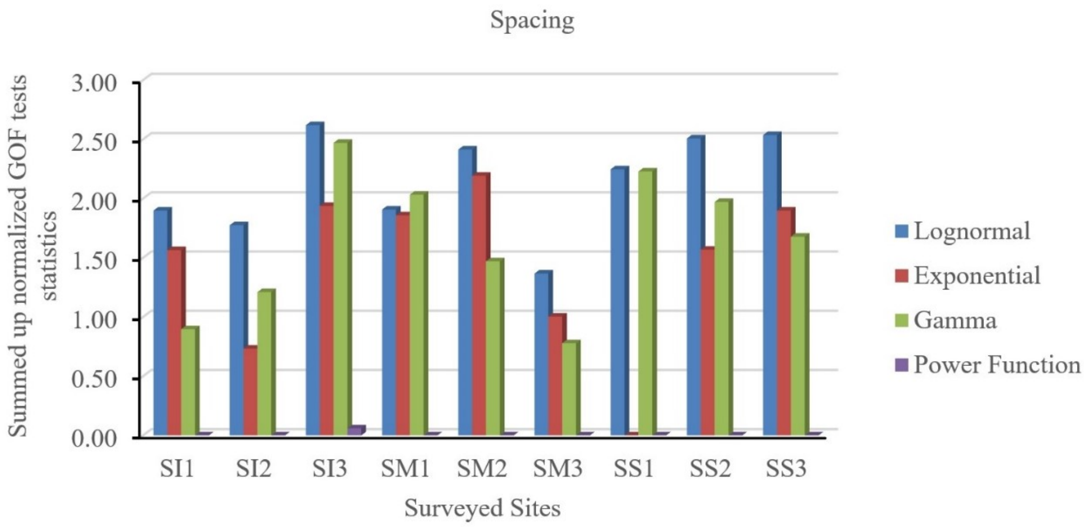

Figure 3. Comparison views of summed up normalized GoF test statistics values for joint spacing of all surveyed exposures.

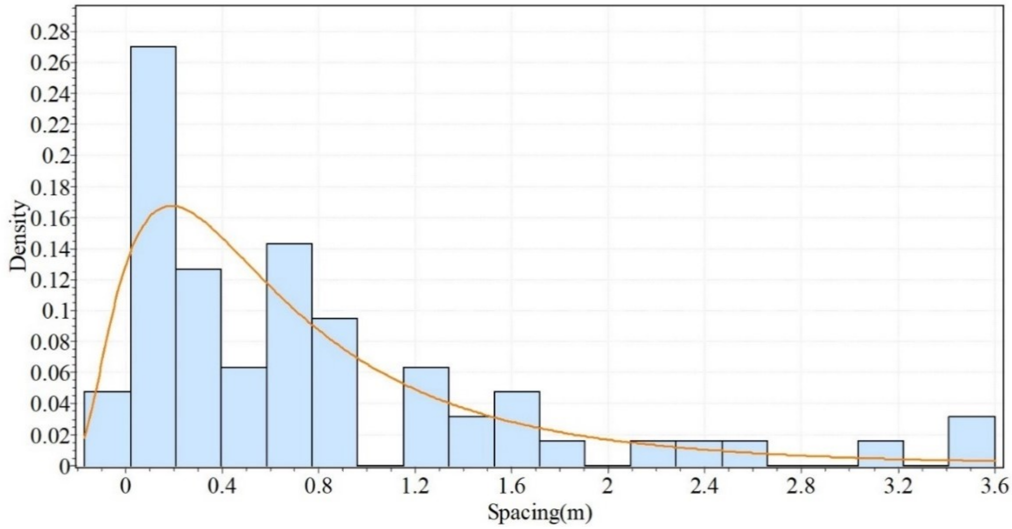

Figure 4. Lognormal distribution of joint spacing of SI1 outcrops.

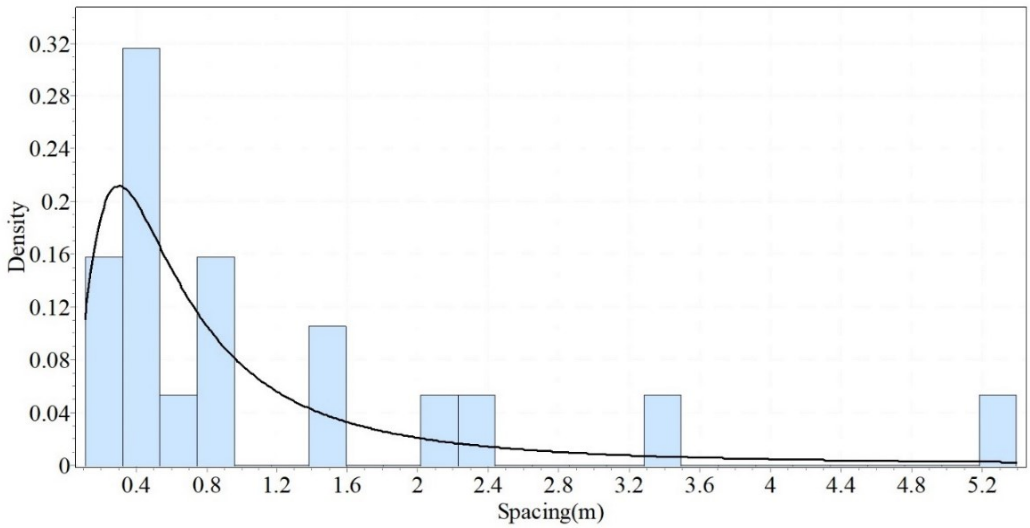

Figure 5. Lognormal distribution of joint spacing of SM2 outcrops.

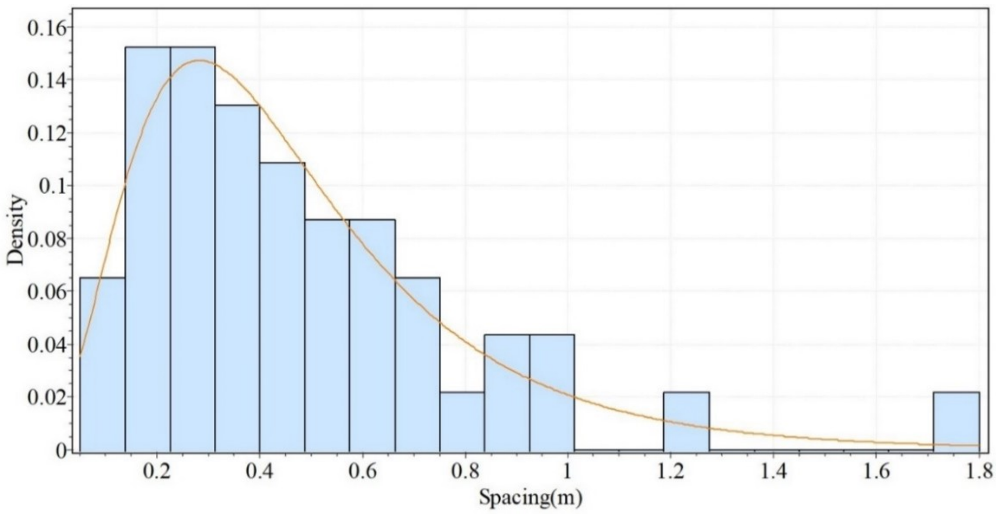

Figure 6. Lognormal distribution of joint spacing of SS1 outcrops.

The result is correct since the rock mass is considered soil if the existing joints are too close. As seen in Figure 4 to Figure, the relative frequency increased by reducing 6, the spacing size. Still, the relative frequency was reduced too by decreasing the spacing size from a specific value. Since we are dealing with rock masses, the relative frequency must be increasing until a certain amount, which describes the lognormal distribution function.

4.2. Joint aperture distribution function

The calculated GoF test statistics of Kolmogorov-Smirnov, Anderson-Darling, and Chi-Squared tests of aperture are shown in Table 4. The comparison views of the summed up normalized GoF test statistics values for a joint aperture of all surveyed exposures are shown in Figure 7. According to the calculated GoF test statistics, the lognormal distribution was the best probability distribution function for representing a joint aperture, established in Equation 8. Also Figure 8 to Figure 10 show three samples of the obtained lognormal distribution function of the joint aperture.

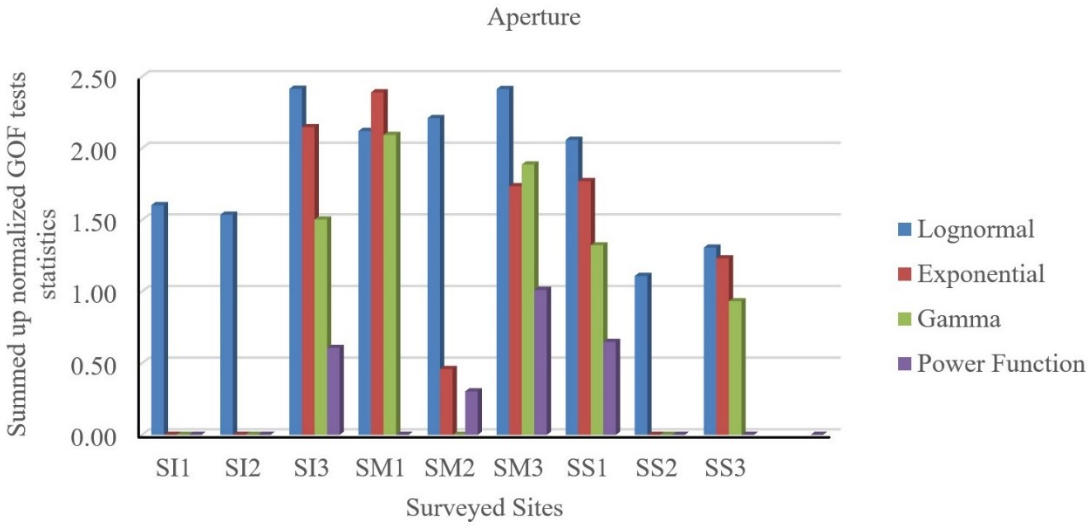

Figure 7. Comparison views of summed up normalized GoF test statistics values for a joint aperture of all surveyed exposures.

Table 3. Test statistic of Kolmogorov-Smirnov, Anderson-Darling, and Chi-Squared tests of aperture.

Site	Test statistic																												The best probability distribution function
	Lognormal							Exponential							Gamma							Power Function							
	D	D_c	A^2	A^2_c	x^2	x^2_c	S	D	D_c	A^2	A^2_c	x^2	x^2_c	S	D	D_c	A^2	A^2_c	x^2	x^2_c	S	D	D_c	A^2	A^2_c	x^2	x^2_c	S	
SI1	0.11	0.17	0.85	2.50	4.53	11.1	**1.60**	0.19	0.17	3.50	2.50	9.56	9.49	-0.5	0.24	0.17	2.90	2.50	6.89	11.1	-0.2	0.37	0.17	50.9	2.50	NA	NA		**Lognormal**
SI2	0.13	0.17	0.88	2.50	4.36	12.6	**1.54**	0.25	0.17	5.84	2.50	15.0	12.6	-2.0	0.32	0.17	4.47	2.50	4.67	12.6	-1.0	0.40	0.17	102	2.50	NA	NA		**Lognormal**
SI3	0.11	0.24	0.31	2.50	0.01	7.81	**2.42**	0.15	0.24	0.55	2.50	0.06	7.81	2.15	0.17	0.24	1.35	2.50	1.94	7.81	1.50	0.30	0.24	11.5	2.50	NA	NA		**Lognormal**
SM1	0.10	0.23	0.37	2.50	2.31	7.81	2.12	0.10	0.23	0.34	2.50	0.36	9.49	**2.39**	0.11	0.23	0.34	2.50	2.77	9.49	2.09	0.22	0.23	2.20	2.50	5.15	5.99	0.30	**Exponential**
SM2	0.15	0.29	0.42	2.50	0.62	5.99	**2.21**	0.30	0.29	2.22	2.50	3.70	5.99	0.46	0.35	0.29	2.45	2.50	9.29	5.99	-0.7	0.31	0.29	2.16	2.50	0.21	3.84	1.01	**Lognormal**
SM3	0.11	0.31	0.31	2.50	0.64	5.99	**2.41**	0.21	0.31	0.82	2.50	1.55	5.99	1.74	0.19	0.31	0.69	2.50	1.34	5.99	1.89	0.27	0.31	8.87	5.99	NA	NA		**Lognormal**
SS1	0.09	0.19	0.79	2.50	1.43	9.49	**2.06**	0.09	0.19	0.51	2.50	5.23	9.49	1.77	0.13	0.19	1.07	2.50	6.25	11.1	1.32	0.18	0.19	5.58	2.50	NA	NA		**Lognormal**
SS2	0.22	0.31	1.55	2.50	3.36	5.99	**1.11**	0.28	0.17	6.44	2.50	15.1	9.49	-2.8	0.41	0.17	9.46	2.50	24.6	9.49	-5.8	0.39	0.17	16.7	2.50	NA	NA		**Lognormal**
SS3	0.15	0.17	1.84	2.50	0.86	9.49	**1.31**	0.11	0.19	1.28	2.50	6.54	9.49	1.23	0.17	0.19	0.93	2.50	9.35	11.1	0.93	0.16	0.19	3.92	2.50	7.24	9.49	-0.2	**Lognormal**

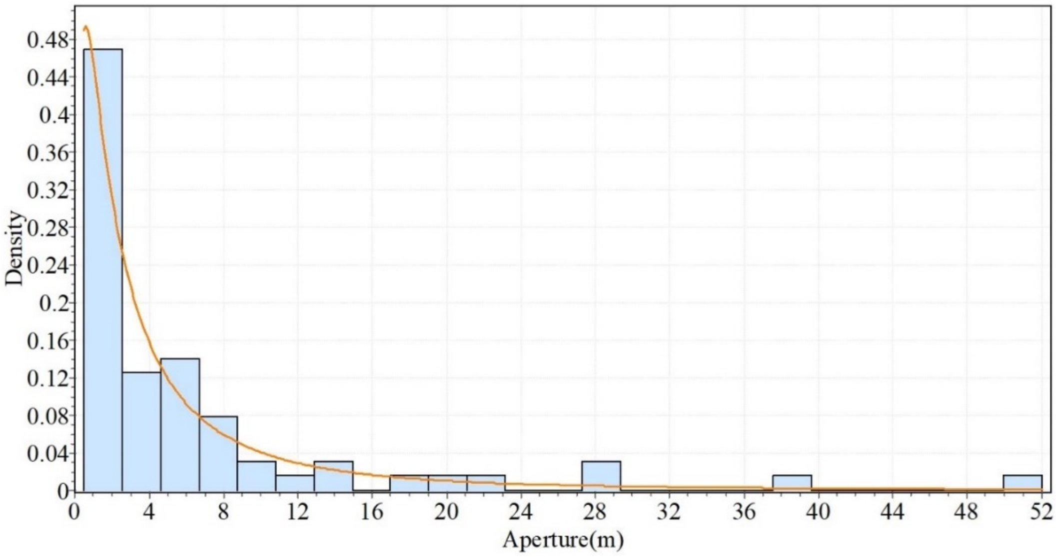

Figure 8. Lognormal distribution of joint aperture of SI1 outcrops.

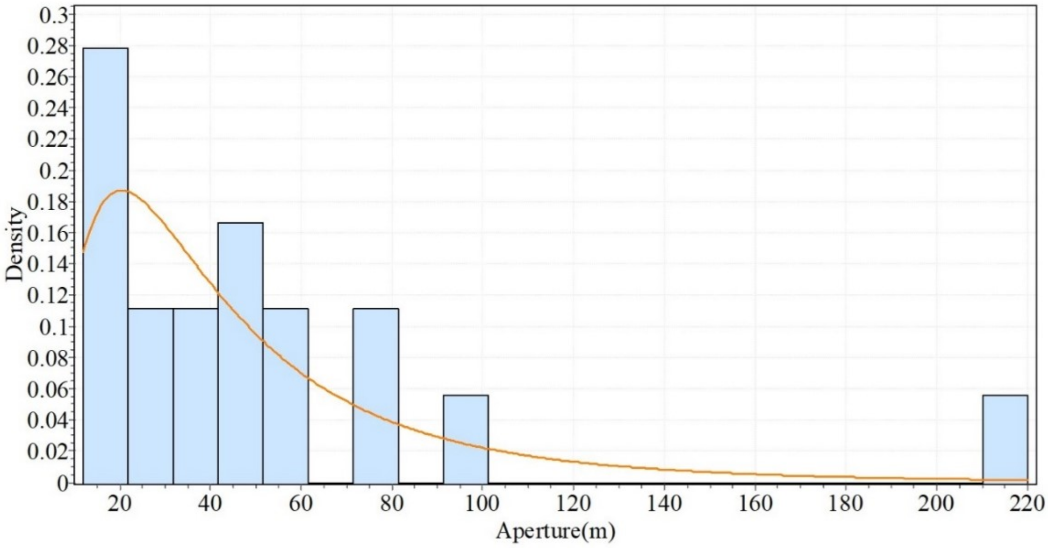

Figure 9. Lognormal distribution of joint aperture of SM3 outcrops.

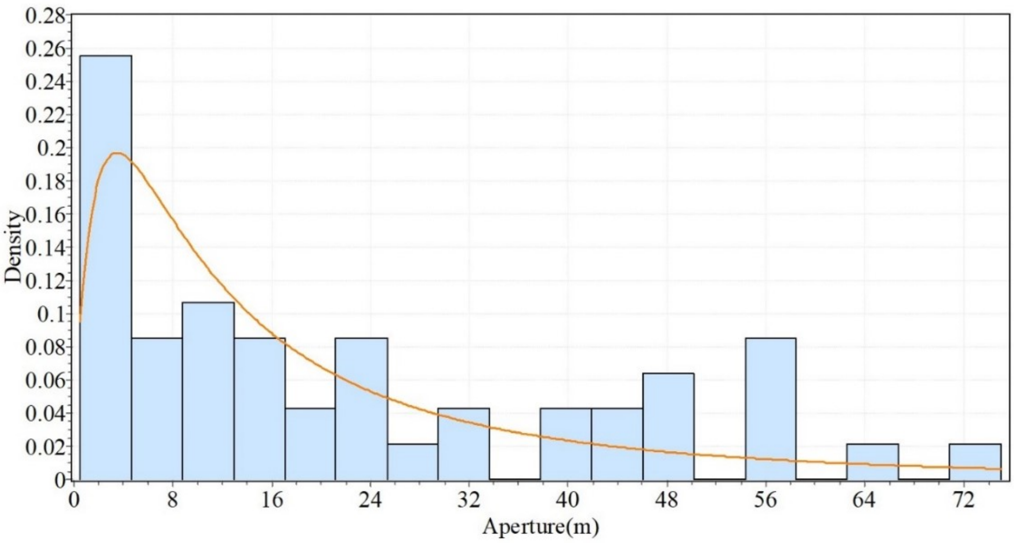

Figure 10. Lognormal distribution of joint aperture of SS1 outcrops.

As explained in the description of the spacing, it was concluded that the joint spacing must follow a lognormal distribution function. A Large opening must have a low frequency, and a small space must have a high frequency. From the inherent nature of the rock, masses can be concluded that by reducing the size of the aperture, the relative frequency increased. Still, from a specific value, the relative frequency must be reduced by reducing the size of the aperture. Since we study the rock mass in macro de, if the opening is too s, mall, it cannot be seen as opening in macro mode, and are not measured. Therefore, the joint aperture must follow the lognormal distribution function.

5.2. Joint orientation distribution function

The calculated GoF test statistics of Kolmogorov-Smirnov, Anderson-Darling, and Chi-Squared tests of dip and dip direction are shown in Table 5 and Table 6. In addition, the comparison views of summed up normalized GoF test statistics values for joint orientation of all surveyed exposures are shown in Figure 11 and Figure 15. The surveyed sites except for the SM3, SS1, and SS2 areas showed the best fit to the Cauchy distribution function according to the calculated GoF test statistics, and it was also found that the Cauchy distribution function was the best probability distribution function to represent the joint dip direction of igneous rocks whose probability density function is defined as Equation 9.

$$f(x)=\left(\pi\sigma\left(1+\left(\frac{x-\mu}{\sigma}\right)^{2}\right)\right)^{-1} \tag{9}$$

where σ is the continuous scale parameter (σ > 0) and μ is the continuous location parameter [95]. Also the Burr distribution functions are the best probability distribution functions to represent the joint dip direction of sedimentary and metamorphic rocks whose probability density function is defined as Equation 10:

$$f(x)=\frac{ak\left(\frac{x}{\beta}\right)^{a-1}}{\beta\left(1+\left(\frac{x}{\beta}\right)^{a}\right)^{k+1}} \tag{10}$$

where k and a are the continuous shape parameter (k and a > 0), and β is the continuous scale parameter (β > 0) [95]. Figure 12, Figure 13, and Figure 14 show three samples of the obtained Cauchy distribution function of joint dip. In addition, Figure 16, Figure 17, and Figure 18 show three samples of the obtained Cauchy and Burr distribution function of dip direction.

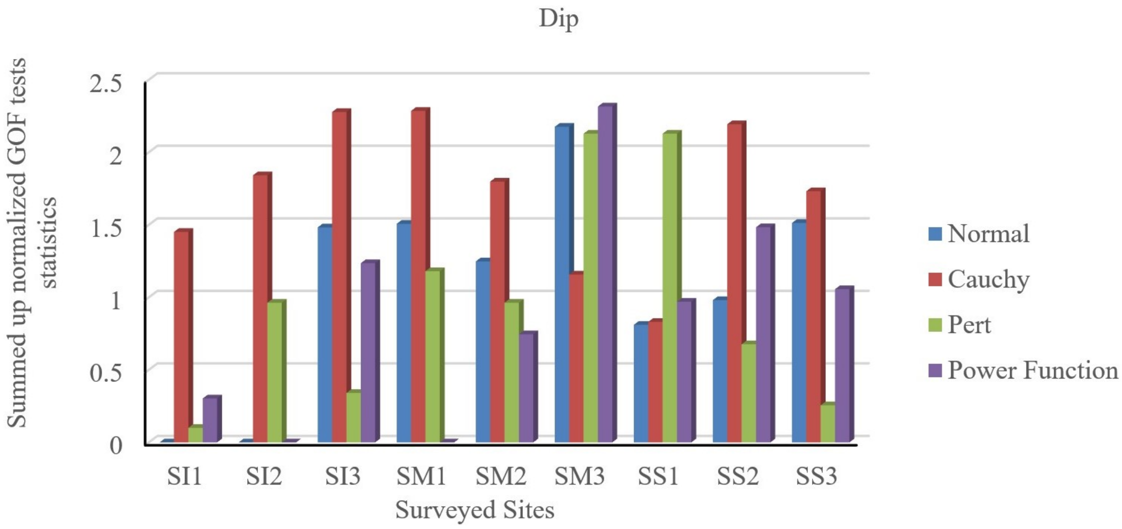

Figure 11. Comparison views of summed up normalized GoF test statistics values for a joint dip of all surveyed exposures.

Table 4. Test statistic of Kolmogorov-Smirnov, Anderson-Darling, and Chi-Squared tests of dip.

Site	Test statistic																												The best probability distribution function
	Normal							Cauchy							Pert							Power Function							
	D	D_c	A^2	A^2_c	x^2	x^2_c	S	D	D_c	A^2	A^2_c	x^2	x^2_c	S	D	D_c	A^2	A^2_c	x^2	x^2_c	S	D	D_c	A^2	A^2_c	x^2	x^2_c	S	
SI1	0.22	0.17	4.26	2.5	22.4	7.81	-2.9	0.13	0.17	1.02	2.5	3.57	9.5	**1.5**	0.14	0.17	3.15	2.5	7.72	9.49	0.1	0.12	0.17	4.72	2.5	0.98	9.49	0.3	Cauchy
SI2	0.22	0.16	4.12	2.5	17.2	11.1	-1.6	0.12	0.16	0.74	2.5	1.24	9.5	**1.8**							NA	0.25	0.16	4.71	2.5	13.2	9.49	-1.8	Cauchy
SI3	0.17	0.24	1.07	2.5	2.98	7.81	1.48	0.12	0.24	0.52	2.5	0.1	7.8	**2.3**	0.16	0.24	2.91	2.5	4.88	5.99	0.34	0.14	0.24	0.87	2.5	4.99	5.99	1.24	Cauchy
SM1	0.14	0.23	0.84	2.5	4.35	7.81	1.51	0.1	0.23	0.48	2.5	0.78	7.8	**2.3**	0.15	0.23	0.84	2.5	6.68	7.81	1.18	0.19	0.23	1.86	2.5	10.2	5.99	-0.3	Cauchy
SM2	0.28	0.29	1.53	2.5	1.21	5.99	1.25	0.17	0.29	0.88	2.5	1.67	6	**1.8**	0.19	0.29	1.34	2.5	5.08	5.99	0.96	0.16	0.29	2.15	2.5	5.18	5.99	0.75	Cauchy
SM3	0.17	0.31	0.65	2.5	0.11	3.84	2.18	0.22	0.31	1.26	2.5	3.74	6	1.2	0.14	0.31	0.62	2.5	1.03	5.99	2.13	0.15	0.31	0.2	2.5	0.77	5.99	**2.3**	Power Functi on
SS1	0.2	0.19	2.08	2.5	3.21	9.49	0.81	0.16	0.19	1.82	2.5	4.89	7.8	0.8	0.1	0.19	0.51	2.5	1.47	11.1	**2.1**	0.16	0.19	1.46	2.5	5.94	9.49	0.97	Pert
SS2	0.12	0.17	1.36	2.5	8.41	11.1	0.98	0.07	0.17	0.28	2.5	3.07	11	2.2	0.16	0.17	1.69	2.5	6.86	9.49	**0.7**	0.09	0.17	0.87	2.5	6.86	11.1	1.48	Pert
SS3	0.11	0.19	1.25	2.5	3.12	7.81	1.51	0.1	0.19	0.53	2.5	5.3	9.5	**1.7**	0.18	0.19	2.4	2.5	6.77	7.81	0.26	0.13	0.17	1.8	2.5	4.42	9.49	1.06	Cauchy

Table 5. Test statistic of Kolmogorov-Smirnov, Anderson-Darling, and Chi-Squared tests of dip direction.

Site	Test statistic																												The best probability distribution function
	Normal							Burr							Cauchy							Pert							
	D	D_c	A^2	A^2_c	x^2	x^2_c	S	D	D_c	A^2	A^2_c	x^2	x^2_c	S	D	D_c	A^2	A^2_c	x^2	x^2_c	S	D	D_c	A^2	A^2_c	x^2	x^2_c	S	
SI1	0.17	0.17	2.41	2.5	14.6	7.81	-0.8	0.17	0.17	5.35	2.5	1.42	7.81	-0.3	0.11	0.17	0.53	2.5	1.42	7.8	**1.9**	0.31	0.17	7.46	2.5	9	7.81	-3	**Cauchy**
SI2	0.21	0.16	2.69	2.5	51.0	9.49	-4.7	0.15	0.24	0.74	2.5	0.51	5.99	2.01	0.13	0.29	0.36	2.5	0.81	6	**2.3**	0.22	0.16	3.01	2.5	27.7	9.49	-2.5	**Cauchy**
SI3	0.18	0.24	1.04	2.5	6.60	5.99	0.72	0.15	0.24	0.82	2.5	1.1	7.81	1.9	0.09	0.24	1.07	2.5	1.02	7.8	**2.1**	0.22	0.24	7.01	2.5	4.53	5.99	-1.5	**Cauchy**
SM1	0.27	0.23	1.54	2.5	6.82	5.99	0.1	0.23	0.23	1.48	2.5	1.17	7.81	**1.3**	0.21	0.23	2.34	2.5	0.64	7.8	1.1	0.27	0.23	7.95	2.5	6.25	5.99	-2.4	**Burr**
SM2	0.15	0.29	0.56	2.5	1.21	3.84	1.96	0.09	0.29	0.24	2.5	0	3.84	**2.6**	0.1	0.29	0.29	2.5	0.24	6	2.5	0.13	0.29	3.02	2.5	0.38	5.99	1.29	**Burr**
SM3	0.24	0.31	1.05	2.5	2.23	3.84	1.23	0.14	0.31	0.46	2.5	0.51	5.99	**2.3**	0.19	0.31	0.53	2.5	4.42	6	1.4	0.2	0.31	2.34	2.5	1.3	5.99	1.19	**Burr**
SS1	0.26	0.19	3.35	2.5	29.6	7.81	-3.4	0.13	0.19	1.15	2.5	6.41	9.49	**1.2**	0.24	0.23	1.73	2.5	1.23	6	1.1	0.31	0.19	26.8	2.5	20.7	5.99	-13	**Burr**
SS2	0.21	0.17	3.69	2.5	21.1	7.81	-2.4	0.1	0.29	0.39	2.5	0.54	5.99	**2.4**	0.24	0.31	0.81	2.5	7.4	6	0.7	0.25	0.17	4.85	2.5	23.1	7.81	-3.3	**Burr**
SS3	0.23	0.19	3.58	2.5	22.8	9.49	-1.9	0.15	0.24	1.06	2.5	0.86	3.84	**1.7**	0.18	0.29	5.77	2.5	3.38	6	-0.5	0.23	0.19	1.75	2.5	17.3	7.81	-1.1	**Burr**

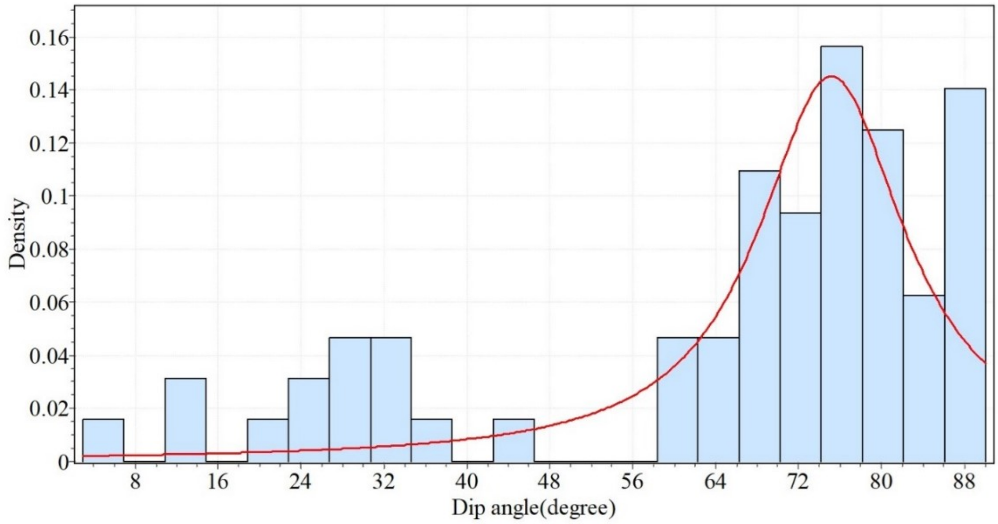

Figure 12. Cauchy distribution of joint dip angle of SI1 outcrops.

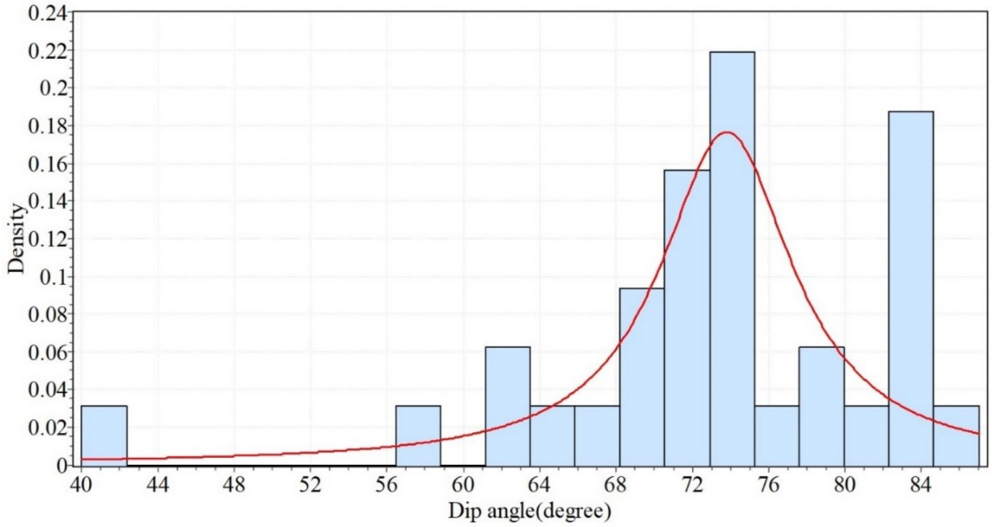

Figure 13. Cauchy distribution of joint dip angle of SM1 outcrops.

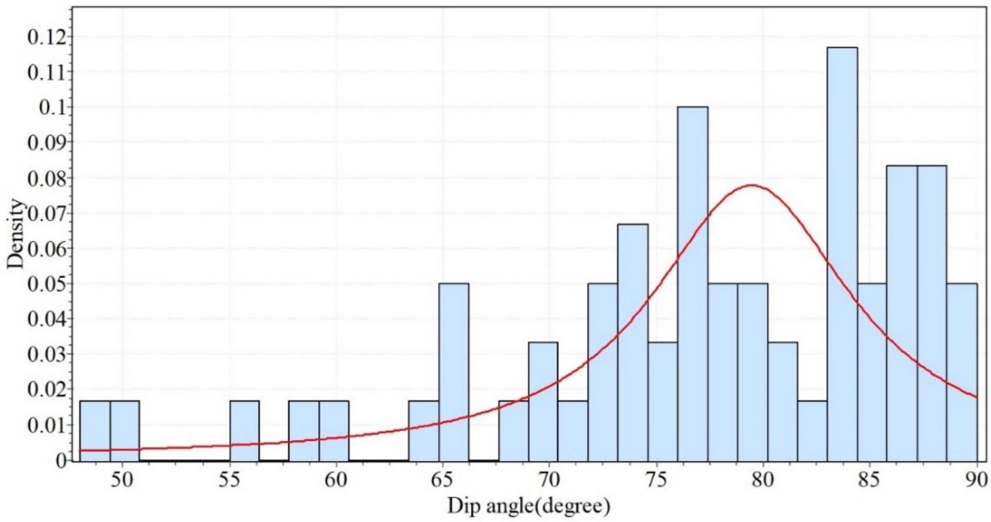

Figure 14. Cauchy distribution of joint dip angle of SS2 outcrops.

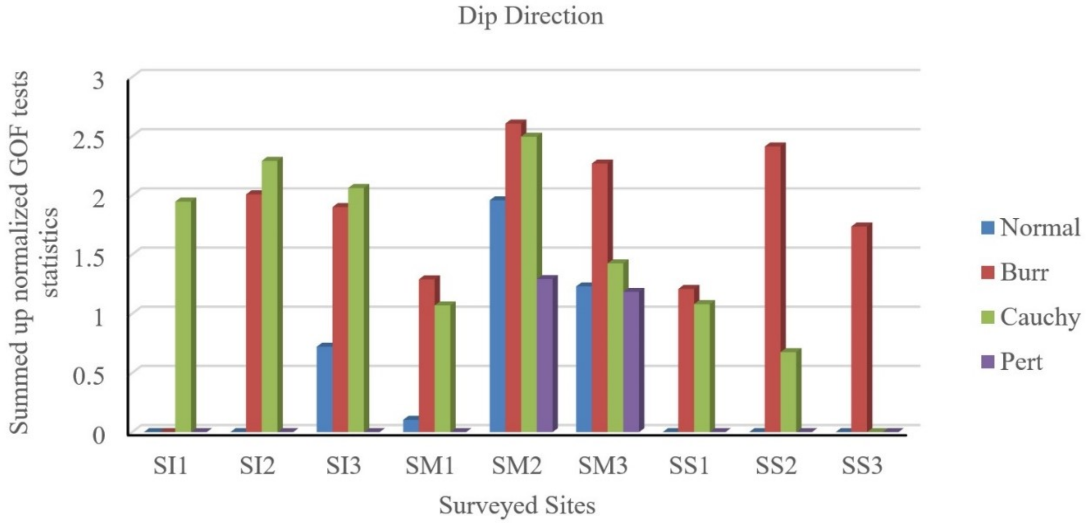

Figure 15. Comparison views of summed up normalized GoF test statistics values for joint dip direction of all surveyed exposures.

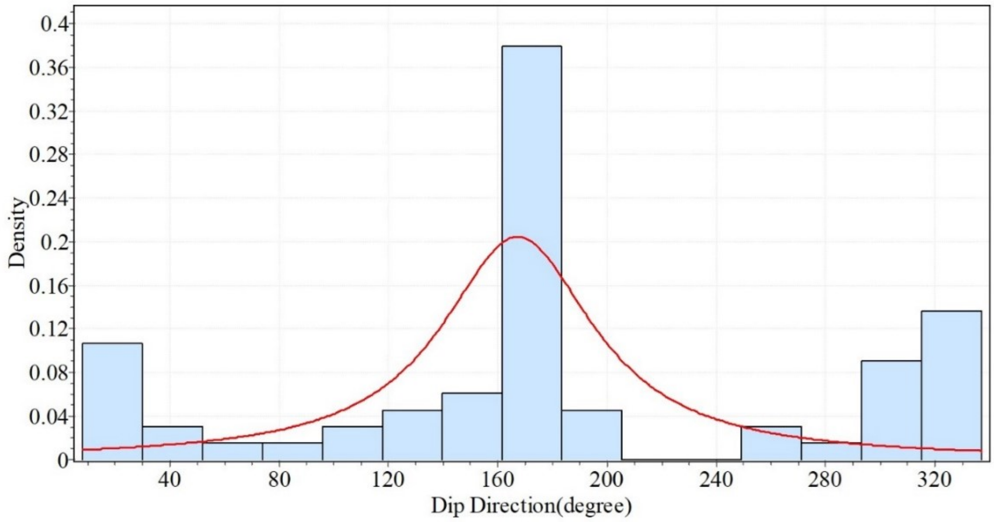

Figure 16. Cauchy distribution of joint dip direction of SI2 outcrops.

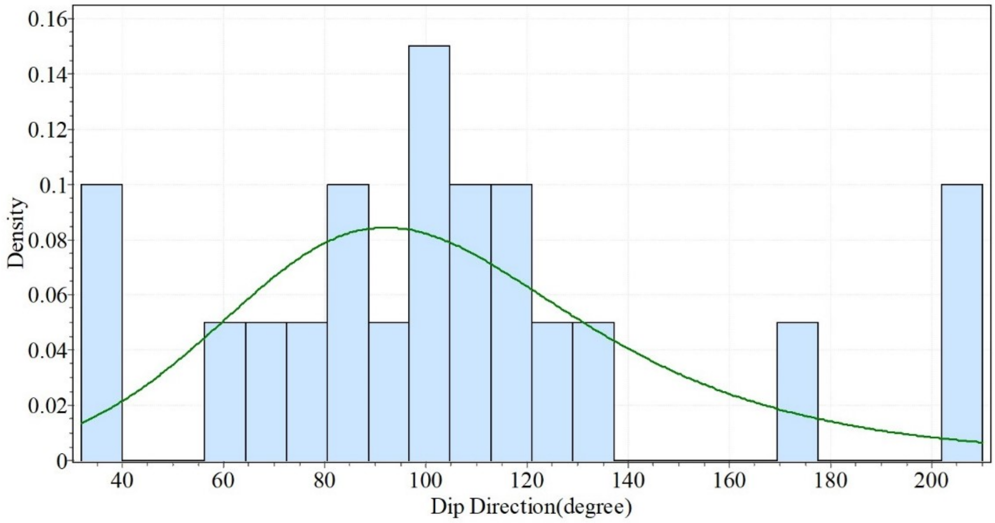

Figure 17. Burr distribution of joint dip direction of SM2 outcrops.

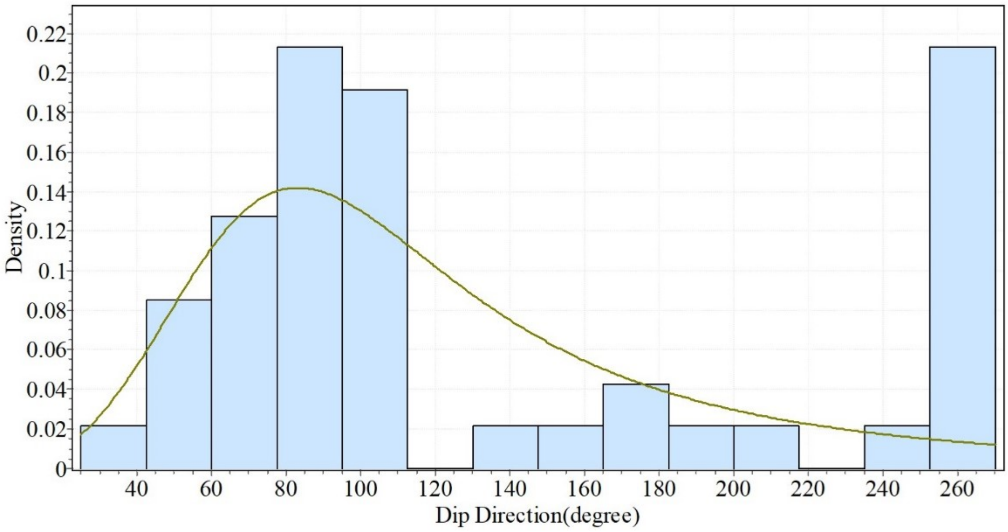

Figure 18. Burr distribution of joint dip direction of SS1 outcrops.

5.3. Joint trace length distribution function

The calculated GoF test statistics of the Kolmogorov-Smirnov, Anderson-Darling, and Chi-Squared tests of observed trace length and estimated trace length by SVM are shown in Table 7. By comparing the GoF test statistic values for the obtained trace length in all sites, it is essential to determine which GoF test statistic value of estimated trace length by SVM is smaller than the observed trace length for the lognormal distribution function. The comparison of these results shows that if most of the existing joints in the exposure are obscured, the distributions will not be determined from the best fit of a functional form to the observed, collected field data. This clearly shows that it is essential to consider the trace length prediction by the learning models such as SVM when estimating the actual trace length distribution function. The comparison views of summed up normalized GoF test statistics values for joint trace length of all surveyed exposures are shown in Figure 19 and Figure 20.

According to the calculated GOF test statistics, the lognormal distribution was the best probability distribution to represent a joint trace length distribution, shown in Equation 8. Also Figure 21, Figure 22, and Figure 23 show three samples of the obtained lognormal distribution of estimated joint trace length by the SVM model.

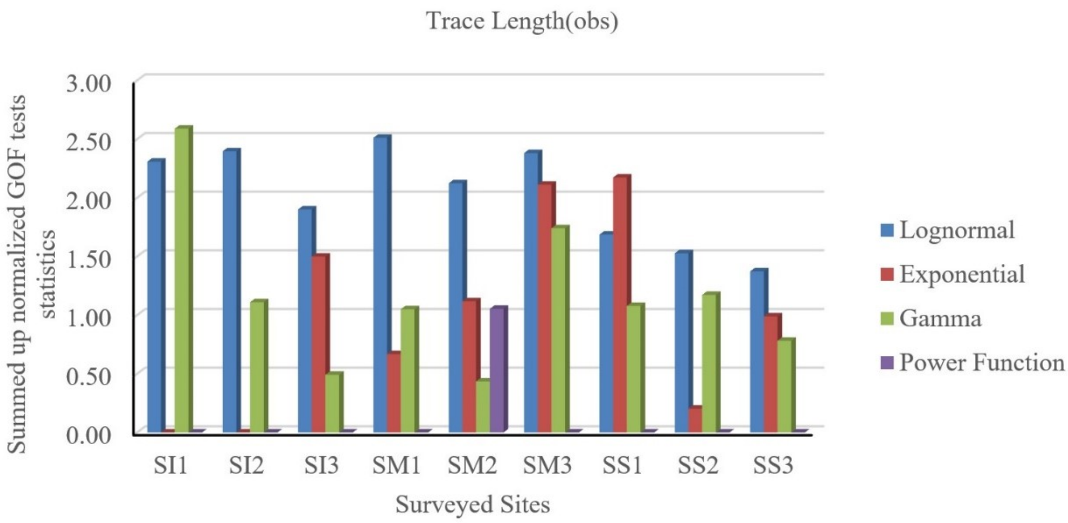

Figure 19. Comparison views of summed up normalized GoF test statistics values for joint trace length (obs) of all surveyed exposures.

Table 6. Test statistic of Kolmogorov-Smirnov, Anderson-Darling, and Chi-Squared tests of observation trace length.

Site	Test statistic																												The best probability distribution function
	Lognormal							Exponential							Gamma							Power Function							
	D	D_c	A^2	A^2_c	x^2	x^2_c	S	D	D_c	A^2	A^2_c	x^2	x^2_c	S	D	D_c	A^2	A^2_c	x^2	x^2_c	S	D	D_c	A^2	A^2_c	x^2	x^2_c	S	
SI1	0.07	0.17	0.46	2.50	1.06	11.1	2.31	0.19	0.17	3.92	2.50	15.3	11.1	-1.1	0.04	0.17	0.16	2.50	1.23	11.1	**2.59**	0.17	0.17	3.08	2.50	20.1	7.81	-1.8	Gamma
SI2	0.06	0.17	0.31	2.50	1.59	12.6	**2.40**	0.16	0.17	2.66	2.50	16.7	11.1	-0.5	0.10	0.17	1.14	2.50	10.6	12.6	1.11	0.20	0.17	8.30	2.50	NA	NA	NA	Lognormal
SI3	0.15	0.24	0.42	2.50	2.39	7.81	**1.90**	0.19	0.24	1.08	2.50	1.66	5.99	1.50	0.20	0.24	1.62	2.50	6.15	5.99	0.49	0.26	0.24	6.51	2.50	NA	NA	NA	Lognormal
SM1	0.09	0.24	0.25	2.50	0.08	5.99	**2.51**	0.17	0.24	1.36	2.50	6.47	5.99	0.67	0.16	0.24	1.22	2.50	6.21	7.81	1.05	0.35	0.24	8.47	2.50	NA	NA	NA	Lognormal
SM2	0.13	0.29	0.28	2.50	1.89	5.99	**2.12**	0.23	0.29	1.27	2.50	3.48	5.99	1.12	0.30	0.29	1.83	2.50	4.78	5.99	0.44	0.32	0.29	2.10	2.50	0.01	3.84	1.05	Lognormal
SM3	0.12	0.31	0.22	2.50	0.86	5.99	**2.38**	0.15	0.31	0.48	2.50	1.27	5.99	2.11	0.21	0.31	1.15	2.50	0.73	5.99	1.74	0.31	0.31	5.82	2.50	NA	NA	NA	Lognormal
SS1	0.15	0.19	0.77	2.50	2.05	9.49	1.69	0.12	0.19	0.10	2.50	1.47	9.49	**2.17**	0.14	0.19	0.87	2.50	7.94	9.49	1.08	0.23	0.19	7.32	2.50	NA	NA	NA	Exponential
SS2	0.11	0.17	0.98	2.50	4.11	9.49	**1.53**	0.18	0.17	1.96	2.50	10.6	11.1	0.20	0.14	0.17	1.45	2.50	4.02	9.49	1.17	0.17	0.17	6.60	2.50	NA	NA	NA	Lognormal
SS3	0.13	0.19	0.68	2.50	6.42	9.49	**1.37**	0.13	0.24	1.35	2.50	7.22	7.81	0.99	0.22	0.29	0.94	2.50	6.55	5.99	0.78	0.14	0.17	5.71	2.50	NA	NA	NA	Lognormal

Table 7. Test statistic of Kolmogorov-Smirnov, Anderson-Darling, and Chi-Squared tests of estimated trace length by SVM.

Site	Test statistic																												The best probability distribution function
	Lognormal							Exponential							Gamma							Power Function							
	D	D_c	A^2	A^2_c	x^2	x^2_c	S	D	D_c	A^2	A^2_c	x^2	x^2_c	S	D	D_c	A^2	A^2_c	x^2	x^2_c	S	D	D_c	A^2	A^2_c	x^2	x^2_c	S	
SI1	0.09	0.17	0.26	2.50	3.27	11.1	**2.07**	0.13	0.17	2.15	2.50	11.3	11.1	0.35	0.15	0.17	2.44	2.50	12.4	11.1	0.02	0.31	0.17	14.1	2.50	NA	NA	NA	Lognormal
SI2	0.07	0.17	0.32	2.50	2.53	12.6	**2.26**	0.12	0.17	1.87	2.50	11.2	11.1	0.53	0.27	0.17	6.42	2.50	34.5	11.1	-4.3	0.26	0.17	13.6	2.50	NA	NA	NA	Lognormal
SI3	0.10	0.24	0.31	2.50	2.97	7.81	**2.08**	0.12	0.24	0.69	2.50	2.50	5.99	1.81	0.18	0.24	1.26	2.50	4.52	7.81	1.17	0.26	0.24	6.65	2.50	NA	NA	NA	Lognormal
SM1	0.11	0.24	0.31	2.50	0.54	7.81	**2.35**	0.19	0.24	1.42	2.50	4.73	7.81	1.03	0.16	0.24	1.09	2.50	1.47	5.99	1.65	0.26	0.24	6.92	2.50	NA	NA	NA	Lognormal
SM2	0.15	0.29	0.43	2.50	1.94	5.99	**1.99**	0.33	0.29	3.12	2.50	9.81	3.84	-1.9	0.35	0.29	2.33	2.50	5.42	5.99	-0.0	0.31	0.29	1.97	2.50	0.25	3.81	1.08	Lognormal
SM3	0.13	0.31	0.25	2.50	0.85	5.99	**2.34**	0.16	0.31	0.52	2.50	1.27	5.99	2.06	0.20	0.31	1.07	2.50	0.66	5.99	1.82	0.30	0.31	5.69	2.50	NA	NA	NA	Lognormal
SS1	0.09	0.19	0.64	2.50	0.49	9.49	**2.22**	0.10	0.19	0.70	2.50	0.86	11.1	2.12	0.14	0.19	0.67	2.50	3.91	9.49	1.58	0.16	0.19	5.16	2.50	NA	NA	NA	Lognormal
SS2	0.13	0.17	1.23	2.50	3.10	9.49	**1.42**	0.27	0.17	5.85	2.50	15.5	9.49	-2.6	0.44	0.17	11.9	2.50	25.8	9.49	-7.1	0.37	0.17	13.7	2.50	NA	NA	NA	Lognormal
SS3	0.10	0.17	0.44	2.50	3.42	11.1	**1.95**	0.24	0.31	1.55	2.50	3.29	3.84	0.76	0.27	0.24	7.35	2.50	23.2	5.99	-4.9	0.28	0.24	5.18	2.50	2.72	5.99	-0.7	Lognormal

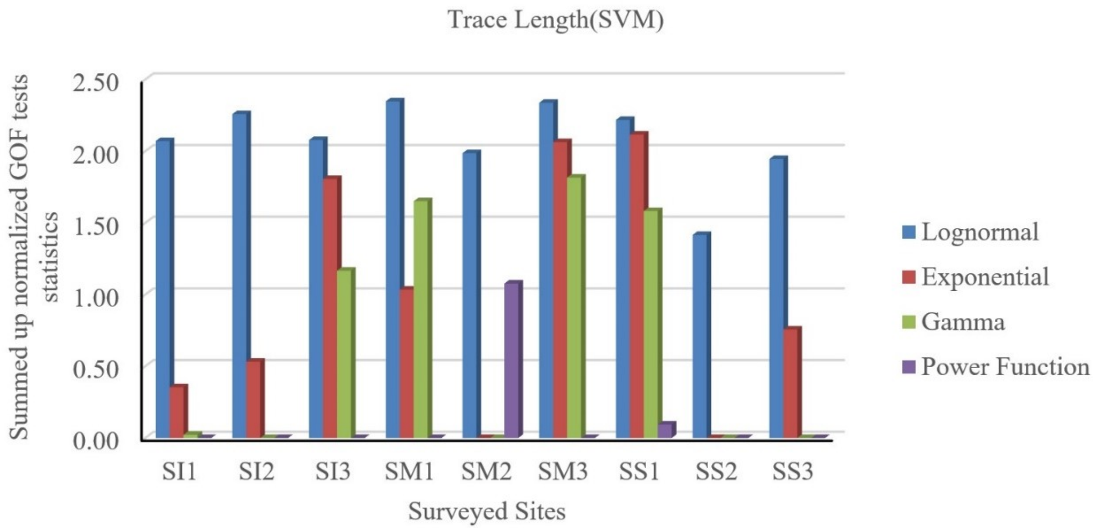

Figure 20. Comparison views of summed up normalized GoF test statistics values for joint trace length (SVM) of all surveyed exposures.

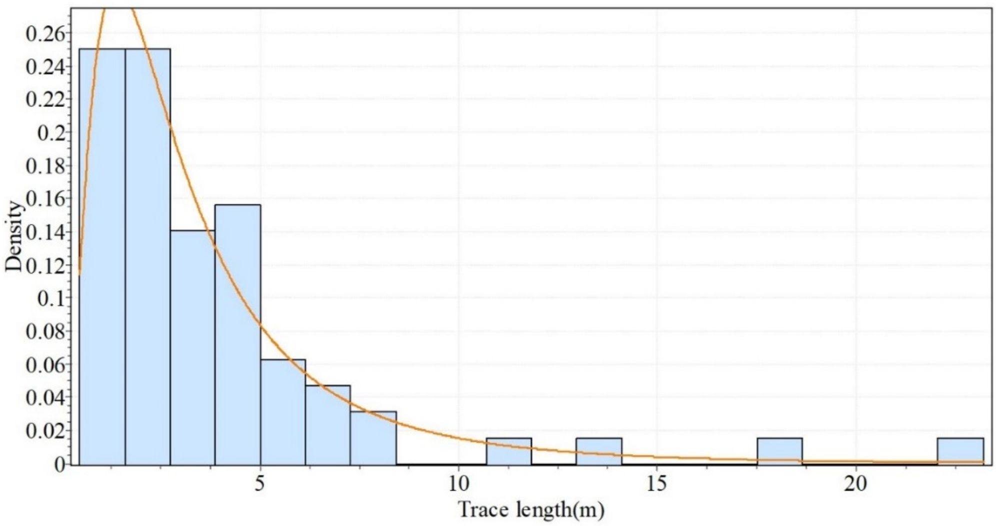

Figure 21. Lognormal distribution of joint trace length of SI2 outcrops.

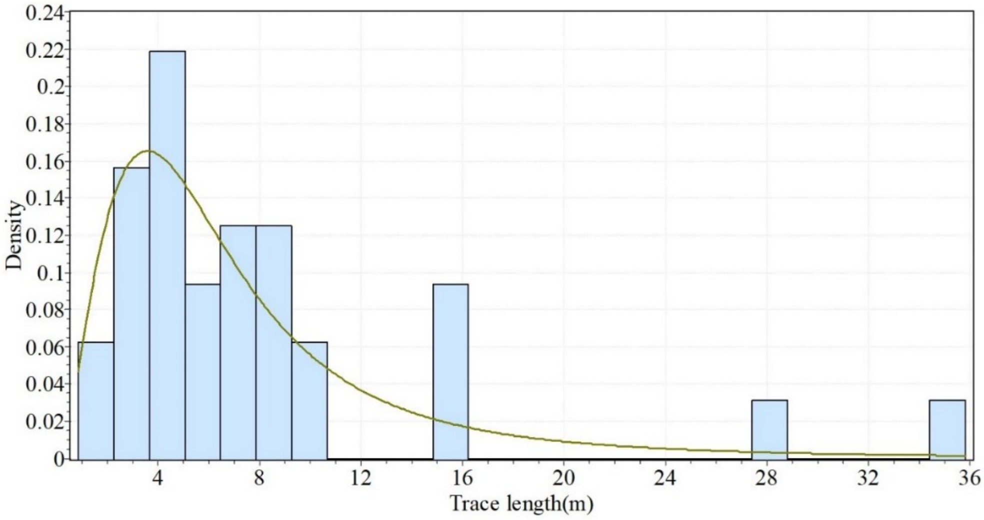

Figure 22. Lognormal distribution of joint trace length of SM1 outcrops.

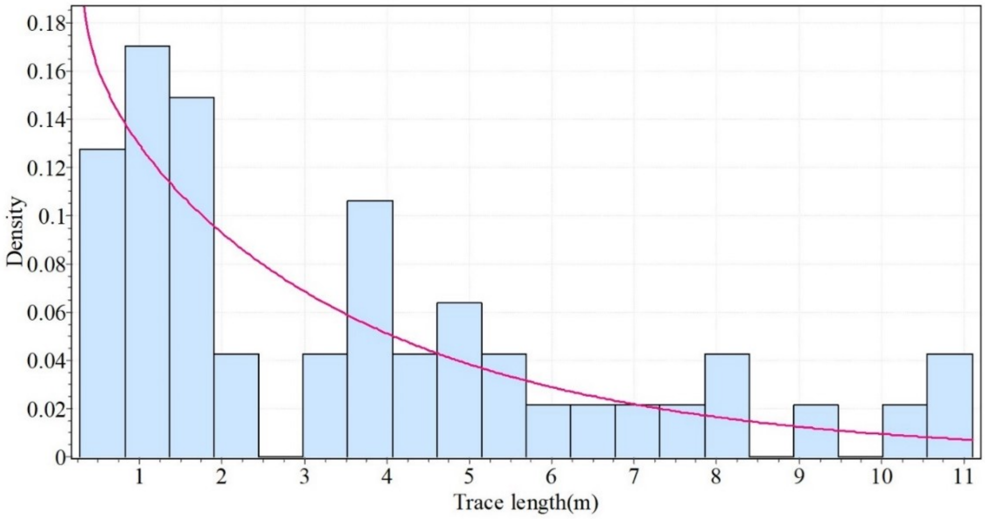

Figure 23. Lognormal distribution of joint trace length of SS1 outcrops.

As mentioned earlier, it was concluded that the joints' spacing and aperture due to their inherent nature must follow a lognormal distribution function. Similar to the spacing and aperture of joints, it is clear that a considerable trace length of joints must have a low frequency, and a small trace length must have a high frequency. Also from the inherent nature of the rock masses, it could be concluded that by reducing the size of trace length, the relative frequency increased. Still, the relative frequency must be reduced from a specific value by reducing the size of the trace length. Since we study the rock mass in the macro mode, if the trace length is too small, it cannot be seen as a trace length in the macro mode, and they are not measured. Therefore, similar to the spacing and aperture, the joint trace length must follow a lognormal distribution function.

6. Conclusions

Since the properties of the joints typically vary over a wide range, their nature of random characteristics is required to be appropriately described in the preliminary design investigations. Therefore, due to the existence of vast areas of the potential application of probabilistic methods in geo-sciences, the natural phenomena occur with such a variation that a stochastic rather than a deterministic system definition is more realistic. However, it is possible to consider the full range of data concerning the specific random characteristics in a stochastic estimation. This can be easily achieved with the probability distributions, which give both the range of values that the variable could take and the relative frequency of each value within the range.

Due to the inherent statistical nature of the joint properties, its geometry should be characterized statistically. The joints have short lengths but are many, and have not been displaced previously. Henceforth, in this work, efforts have been made in order to determine the probability distribution function of the rock joint geometry properties. Thus for this purpose, a scanline sampling was surveyed on the rock exposures, and the joint geometry properties (spacing, aperture, orientation (dip and dip direction), roughness, Schmidt rebound of the joint's wall, type of joint termination, joint trace lengths in both sides of the scanline and joint sets) was measured. The Goodness-of-Fit (GoF) tests were applied on the joint geometry properties data obtained in nine outcrops of three rock-type surveys. The GoF test statistics of the Kolmogorov-Smirnov, Anderson-Darling, and Chi-Squared tests of the related probability distribution functions of each joint geometry properties were calculated. In order to minimize the weaknesses and amplify the strength of these three methods, we summed the results together. Then three normalized values of the three GoF tests for each distribution function were added. Consequently, the distribution function with a greater value is the best probability distribution function for representing the joint geometry properties. According to the conducted analyses, the main conclusions of this work are as follow:

i. It could be concluded that the GoF tests satisfied the compatibility of the obtained joint aperture, spacing, and trace length data with a theoretical lognormal probability distribution.

ii. If most of the existing joints in the exposure are obscured, the observed mean trace length will not be a good indicator of the mean trace length of the joints, and the distributions will not be determined from the best fit of a functional form the observed, collected field data.

iii. The surveyed sites except for SM3, SS1, and SS2 showed the best fit to the Cauchy distribution function to represent the joint dip distribution function. The Cauchy distribution function is the best probability distribution function to represent the joint dip direction of igneous rocks. The Burr distribution functions are the best probability distribution function to define the joint dip direction of sedimentary metamorphic rocks.

7. Acknowledgments

The authors would like to thank all the persons for their help in collecting the joint geometry properties.

8. Funding

The authors received no financial support for this article's research work, authorship, and publication.

References

[1]. Hancock, P. (1995). Brittle micro tectonics: principles and practice. Journal of Structural Geology, 7(3,4), 437-457.

[2]. Hudson, J.A. and Harrison, J.P. (1997). Engineering Rock Mechanics: An Introduction to the Principles. Elsevier, Oxford.

[3]. Priest, D.S. (1993). Discontinuity analysis for rock engineering. London: Chapman & Hall.

[4]. Oda, M. A. (1988). method for evaluating the representative elementary volume based on joint survey of rock mass. Can Geotech, 25, 440-447.

[5]. Adler, P.M. and Thovert. J.F. (1999). Fractures and Fracture Networks. Kluwer, Dordrecht. Netherlands.

[6]. Tsang, C.F. and Neretnieks. I. (1998). Flow channeling in heterogeneous fractured rocks. Rev Geophys, 36, 275-298.

[7]. Sahimi, M. (1995). Flow and Transport in Porous Media and Fractured Rock. New York: VCH.

[8]. Bour, O., Davy, P. and Darcel. C. (2002). A statistical scaling model for fracture network geometry, with validation on a multiscale mapping of a joint network (Hornelen Basin, Norway). Geophys Res, 107(B6),10.1029/2001JB000176.

[9]. Darcel, C., Bour, O., Davy, P. and de Dreuzy. J.R. (2003). Connectivity properties of two-dimensional fractures networks with stochastic fractal correlation. Water Resour Res, 39(10), 1272, doi:10.1029/2002WR001628.

[10]. de Dreuzy, J.R. and Erhel. J. (2003). Efficient algorithms for the determination of the connected fracture network and the solution of the steady-state flow equation in fracture networks-short notes. Comp Geosci, 29, 107-111.

[11]. de Dreuzy, J. R., Darcel C, C., Davy P, P., & Bour, O. (2004). Influence of spatial correlation fracture centers on the permeability of two-dimensional fracture networks following a power law length distribution. Water Resour Res, 40, W01502, doi:10.1029/2003WR002260.

[12]. Mourzenko, V.V., Thovert, J.F. and Adler, P. M. (2004). Macroscopic permeability of three-dimensional networks with power-law size distribution. Phys Rev, E (69): 066307,1-13.

[13]. Kulatilake, P., Wang, S. and Stephenson, O. (1993). Scale effects of the deformability of jointed rock at the three-dimensional level. In P. d. Cunha (Ed.), Scale Effects in Rock Masses 93. Lisbon.

[14]. Welideniya, H.S. (2005). Laboratory evaluation and modeling of shear strength of infilled joints under constant normal stiffness (CNS) conditions. Australia: Univ. Wollongong.

[15]. Wang, x.B. (2007). Effect of joint width on strength, stress-strain curve and strain localization of rock mass in uniaxial plane strain compression. Key Eng Maters, 353-358, 1129-1132.

[16]. Baghbanan, A. (2008). Scale And Stress Effects on Hydro-Mechanical Properties of Fractured Rock Masses. Trita-Lwr Ph.D. 1040, KTH land and water resources engineering.

[17]. Meyer, T. and Einstein, H.H. (2002). Geologic Stochastic Modeling and Connectivity Assessment of Fracture Systems in the Boston Area. Rock Mechanics and Rock Engineering, 35(1), 23–44.

[18]. Odling, N.E., Gillespie, P., Bourgine, B., Castaing, C., Chiles, J.-P., Christensen, N.P., Watterson, J. (1999). Variations in fracture system geometry and their implications for fluid flow in fractured hydrocarbon reservoir. Petroleum Geoscience, 5, 373-384.

[19]. Mohamad Javad, A., Abdolhadi, G. and Seyed Amirasad, F. (2021). A new peak shear strength criterion of three-dimensional rock joints considering the scale effects. Arabian Journal of Geosciences, 14(936). doi: https://doi.org/10.1007/s12517-021-07319-5.

[20]. Yingchun, L., Chun'an, T. and Chuangzhou, W. (2020). A New Shear Strength Criterion of Three-Dimensional Rock Joints. Rock Mechanics and Rock Engineering, 53, 1477-1483.

[21]. Miao, C., Sheng-Qi, Y., Pathegama Gamage, R. and Yuan-Chao, Z. (2021). Cracking behavior of rock containing non-persistent joints with various joints inclinations. Theoretical and Applied Fracture

Mechanics, 109. doi:https://doi.org/10.1016/j.tafmec.2020.102701.

[22]. Alejandro, C., Thomas, F. and Carlos, S. (2021). Natural Rock Fractures: From Aperture to Fluid Flow. Rock Mechanics and Rock Engineering, 54, 5827-5844.

[23]. Ameneh f, D., & Rasoul, A. (2015). Evaluation of Hydraulic Aperture of the Joints of Behesht Abad Dam Foundation, Iran. Geology, 5(6), 7.

[24]. Gaojian, H. and Gang, M. (2021). Size effect of parallel-joint spacing on uniaxial compressive strength of rock. doi: https://doi.org/10.1371/journal.pone.0257245.

[25]. Wentao, X., Yangsong, Z., Xiaozhao, L., Xinyong, W., Fei, M. and Jiabin, Z. (2020). Extraction and statistics of discontinuity orientation and trace length from typical fractured rock mass: A case study of the Xinchang underground research laboratory site, China. Engineering Geology, 269. doi: https://doi.org/10.1016/j.enggeo.2020.105553.

[26]. Jiateng, G., Yinhe, L., Lixin, W., Shanjun, L., Tianhong, Y., Wancheng, Z. and Zirui, Z. (2019). A geometry- and texture-based automatic discontinuity trace extraction method for rock mass point cloud. International Journal of Rock Mechanics and Mining Sciences. doi: https://doi.org/10.1016/j.ijrmms.2019.104132.

[27]. Jiayao, C., Mingliang, Z., Hongwei, H., Dongming, Z., & Zhicheng, P. (2021). Automated extraction and evaluation of fracture trace maps from rock tunnel face images via deep learning. International Journal of Rock Mechanics and Mining Sciences. doi: https://doi.org/10.1016/j.ijrmms.2021.104745.

[28]. Hammah, R., Yacouh, T. and Curran, J. (January 4-10, 2009). Numerical Modelling of Slope Uncertainty Due to Rock Mass Jointing. International Conference on Rock Joints and Jointed Rock Masses. Tucson, Arizona, USA.

[29]. Sari, M. (2009). the stochastic assessment of strength and deformability characteristics for a pyroclastic rock mass. International Journal of Rock Mechanics & Mining Sciences, 46, 613–626.

[30]. Muspratt, M. A. (1972). Numerical statistics in engineering geology. Engineering Geology, 6, 67–78.

[31]. Evans, E., Hastings, N. and Peacock, B. (1993). Statistical Distributions (second ed.). New York: John Wiley & Sons.

[32]. Gumede, H. and Stacey, T.R. (2007). Measurement of typical joint characteristics in South African gold mines and the use of these characteristics in the prediction of rock falls. The Journal of the Southern African Institute of Mining and Metallurgy, 107, 335-344.

[33]. Baecher, G.B. (1983). Statistical analysis of rock mass fracturing. Journal of Mathematical Geology, 15, 329–347.

[34]. Call, R.D., Savely, J.P. and Nicholas, D.E. (1976). Estimation of joint set characteristics from surface mapping data. Monograph on Rock Mechanics Applications in Mining, SME -AIME, 65-73.

[35]. Priest, S.D. and Hudson, J.A. (1976). Discontinuity spacing in rock. International Journal of Rock Mechanics, Mining Sciences & Geomechanics, Abstract, 13, 135-148.

[36]. Wallis, R.F. and King, M.S. (1980). Discontinuity spacings in a crystalline rock. International Journal of Rock Mechanics and Mining Sciences & Geomechanics Abstracts, 17(1), 63-66.

[37]. Snow, D.T. (1970). The frequency and apertures of fractures in rock. International Journal of Rock Mechanics and Mining Sciences & Geomechanics Abstracts. 7 (1): 23-30.

[38]. Stacey, T.R. (1989). Potential rockfalls in conventionally supported stopes- a simple probabilistic approach. S. Afr. Inst. Min, Meall. 89 (4): 111-115.

[39]. Kulatilake, P., Chen, J., Teng, J., Shufan, X., & Pan, G. (1996). Discontinuity Geometry Characterization in a Tunnel Close to the Proposed Permanent Shiplock Area of the Three Gorges Dam site in China. International Journal of Rock Mechanics, Mining Science & Geomechanics Abstract. 33 (3): 255-277.

[40]. Sari, M., Karpuz, C. and Ayday, C. (2010). Estimating rock mass properties using Monte Carlo simulation: Ankara andesites. Computers & Geosciences, 36, 959–969.

[41]. Snow, D.T. (1968). ROCK FRACTURE SPACINGS, OPENINGS, AND POROSITIES. Journal of Soil Mechanics & Foundation Div, 94(SM1), 73-91.

[42]. Baecher, G.B., Lanney, N.A. and Einstein, H.H. (1977). Statistical description of rock properties and sampling. 18th U.S. Symp. on Rock Mech, (p. 5C1.1 5C1.8). Colorado.

[43]. Baecher, G.B. and Lanney, N.A. (1978). trace length biases in joint surveys. 19th U.S. Symp. on Rock Mech, 1, pp. 56-65. Nevada.

[44]. Herget G. (1982). Probabilistic slope design for open-pit mines. Rock Mechanics, 12, 163-178.

[45]. Kulatilake, P., Um, J.-g., Wang, M., Richard, F.E. and Narvaiz, J. (2003). stochastic fracture geometry modeling in 3-D including validations for a part of Arrowhead East Tunnel, California, USA. Engineering Geology, 70, 131–155.

[46]. Judy, E. (2002). some effects of weathering on joints in granitic rocks. Catena, 49, 91-109.

[47]. Barton, C.A. and Zoback, M.D. (1990). Self-similar distribution of macroscopic fractures at depth in crystalline rock in the Cajon Pass scientific drill hole, Rock Joints. (B. &. Stephenson, Ed.) Rotterdam: Balkema.

[48]. Brown, E.T. (1981). ISRM suggested methods: rock characterization, testing and monitoring. London: Pergamon.

[49]. Barton, N. (1983). Application of Q-system and index tests to estimate shear strength and Deformability of rock masses. Proceedings of the international symposium on engineering geology and underground construction, (pp. 51–70).

[50]. Mostafa, S., Yasuhiro, M. and Tetsuro, E. (2008). Rock Joint Surfaces Measurement and Analysis of Aperture Distribution under Different Normal and Shear Loading Using GIS. Rock Mechanics and Rock Engineering, 41(2).

[51]. de Dreuzy, J.R., Davy, P. and Bour, O. (2001). Hydraulic properties of two-dimensional random fracture networks following the power law length distribution 1. Effective connectivity. Water Resour Res, 37(8), 2065-2078.

[52]. de Dreuzy, J.R., Davy P.P. and Bour, O. (2001). Hydraulic properties of two-dimensional random fracture network following a power law length distribution 2. Permeability of networks based on lognormal distribution of aperture. Water Resour Res. 37 (8): 2079-2095.

[53]. Wong T.F., Fredrich J.T. and Gwanmesia G.D. (1989). Crack aperture statistics and pore space fractal geometry of Westerly Granite and Rutland Quartzite: Implication for elastic contact model of rock compressibility. Geophys Res, Vol. 94, No. B4, pp. 10,267-10,278.

[54]. Barton, C.A. and Zoback, M.D. (1992). Self-affine distribution and properties of macroscopic fractures at depth in crystalline rock in the Cajon Pass scientific drill hole. Geophys Res, 97(B4), 5181-5200.

[55]. Clark, M.B., Brantley, S.L. and Fisher, D.M. (1995). Power-law vein-thickness distributions and positive feedback in vein growth. Geology. 23 (11): 975–978.

[56]. Fisher, D.M., Brantley, S.L., Everett, M. and Dzvonik, J. (1995). Cubic fluid flow through a regionally extensive fracture network within the Kodiak accretionary prism. Geophys Res, 100(B7), 12881-12894.

[57]. Belfield, W.C. and Sovich, J. (1995). Fractures statistics from horizontal welbores. Can Pet Technology, 34, 47-50.

[58]. Marrett, R. (1996). Aggregate properties of fracture populations. Struct Geol, 18(2-3), 169-178.

[59]. Gale, J.E. (1987). Comparison of coupled fracture deformation and fluid flow models with direct measurements of fracture pore structure and stress-flow properties. In Farmer/Daemen/Desai/Glass/Neuman (Ed.), 28th US Rock Mech Symp, (pp. 1213-1222). Tucson.

[60]. Dverstop, B. and Andersson, J. (1989). Application of the discrete fracture network concept with field data: Possibilities of model calibration and validation. Water Resour Res, 25, 540-550.

[61]. Cacas, M. C., Ledoux, E., de Marsily, G., Tillie, B., Barbreau, A., Durand, E., Peaudecerf, P. (1990). Modeling fracture flow with a stochastic discrete fracture network: Calibration and validation 1. The flow model. Water Resour Res. 26 (3): 479-489.

[62]. Hakami, E. and Barton, N. (1990). Aperture measurements and flow experiments using transparent replicas of rock joints. In S. O. Barton N (Ed.), Int Symp Rock Joints (pp. 383-390). Balkema: Rotterdam.

[63]. Iwano, M. and Einstein, H.H. (1993). Stochastic analysis of surface roughness, aperture and flow in a single fracture. Int Symp EUROCK '93, (pp. 135-141). Lisbon.

[64]. Johns, R.A., Steude, j.S., Castanier, L.M. and Roberts, P.V. (1993). Nondestructive measurements of fracture aperture in crystalline rock cores using X-ray computed tomography. Geophys Res. 98 (B2): 1889-1900., pp. 1889-1900.

[65]. Hakami, E. and Larsson, E. (1996). Aperture Measurements and Flow Experiments on a Single Natural Fracture. Int J Rock Mech. Min Sci & Geomech Abstr. 33 (4): 395-404.

[66]. Pyrak-Nolte, L.J., Montemagno, C.D. and Nolte, D.D. (1997). Volumetric imaging of aperture distributions in connected fracture networks. Geophy Res Lett. 24 (18): 2343-2346.

[67]. Oron, A. P., & Berkowitz, B. (2001). Flow in rock fractures: The local cubic law assumption re-examined. Water Resour Res, 37(8), 2079-2095.

[68]. Bertels, S.P., DiCarlo, D.A. and Blunt, M.J. (2001). Measurement of aperture distribution, capillary pressure, relative permeability, and in-situ saturation in a rock fracture using computed tomography scanning. Water Resour Res. 37 (3): 649-662.

[69]. Priest, S.D. and Hudson, J.A. (1976). Discontinuity spacing in rock. International Journal of Rock Mechanics, Mining Sciences & Geomechanics, Abstract, 13, 135-148.

[70]. Priest, S.D. and Hudson, J.A. (1981). Estimation of discontinuity spacing and trace length using scanline surveys. International Journal of Rock Mechanics and Mining Sciences & Geomechanics Abstracts, 18(3), 183-197.

[71]. Hudson, J.A. and Priest, S.D. (1983). Discontinuity frequency in rock masses. International Journal of Rock Mechanics, Mining Sciences & Geomechanics, Abstract. 20 (2): 73-89.

[72]. Einstein, H.H. and Baecher, G.B. (1983). probabilistic and statistical methods in engineering geology. Rock mechanics and rock engineering, 16, 39-72.

[73]. Dershowitz, W.S. and Einstein, H.H. (1988). Characterizing rock joint geometry with joint system models. Rock mechanics and rock engineering, 21, 21-51.

[74]. Hakami, E. (1995). Aperture distribution of rock fractures. PhD thesis, Division of Engineering, Royal Institute of Technology, Department of Civil and Environmental Engineering, Stockholm, Sweden.

[75]. Palmstrom, A. (1995). A rock mass characterization system for rock engineering purposes. Norway: Oslo University.

[76]. Baecher G., Lanney N. and Einstein H., (1977b). Statistical descriptions of rock properties and sampling. in 19th U.S. national symposium on rock mechanics, Keystone, Colorado.

[77]. Zadhesh J., Jalali S.-M.E. and Ramazanzadeh A., (2013). Estimation of joint trace length probability distribution function in igneous, sedimentary and metamorphic rocks. Arabian Journal of Geosciences, Vols. DOI 10.1007/s12517-013-0861-1.

[78]. Weiss M., (2008). Techniques for estimating fracture size: A comparison of methods. International Journal of Rock Mechanics and Mining Sciences, Vol. 45, p. 460–466.

[79]. Warburton P.M., (1980). A Stereological Interpretation of Joint Trace Data. International Journal of Rock Mechanics and Mining Sciences, Vol. 17, pp. 181-190.

[80]. Barton, C.M. (1978). Analysis of joint traces. 19th Symp. Rock Mech. Am. Inst. Min. Eng, (pp. 39-40).

[81]. Bridge, M.C. (1976). Presentation of Fracture Data for Rock Mechanics. 2nd Australian-New Zealand Conference on Geomechanics, (pp. 144-148). Brisbane.

[82]. Park, Y.J., de Dreuzy, J.R., Lee KK, K.K. and Berkowitz, B. (2001). Transport and intersection mixing in random fracture networks with power law length distributions. Water Resour Res. 37 (10): 2493-2502.

[83]. Song, J.J. and Lee, C.I. (2001). Estimation of joint length distribution using window sampling. International Journal of Rock Mechanics & Mining Sciences, 38, 519–528.

[84]. Call, R.D., Savely, J.P. and Nicholas, D.E. (1976). Estimation of joint set characteristics from surface mapping data. Monograph on Rock Mechanics Applications in Mining, SME -AIME, 65-73.

[85]. ISRM., (1978). Commission on Standardization of Laboratory and Field Tests: Suggested methods for the quantitative description of discontinuities in rock masses. International Journal of Rock Mechanics & Mining Sciences and Geomechanics Abstract, Vol. 15, pp. 319-368.

[86]. Burges, C. (1998). A tutorial on support vector machines for pattern recognition. Data Mining Knowledge Discovery. 2 (2): 121-167.

[87]. Christiani, V. and Shawe -Taylor, J. (2002). An introduction to support vector machines. Cambridge University Press.

[88]. Vapink, V. (1995). The nature of statistical learning theory. New York: Springer.

[89]. Vapink, V. (1998). Statistical learning theory. New York: Wiley.

[90]. Vapink, V. (1999). The Nature of Statistical Learning Theory. New York, USA: Springer-Verlag.

[91]. Gregory, B.B. (1980). Progressively Censored Sampling of Rock Joint Traces. Mathematic Geology, 12(1).

[92]. Priest, S.D. (1993). Discontinuity analysis for rock engineering. London: Chapman & Hall.

[93]. Christianzangerl, Simon, L. and Erik, E. (2006). Structure, geometry and formation of brittle discontinuities in anisotropic crystalline rocks of the Central Gotthard Massif, Switzerland, Eclogae geol. Helv. 99, 271-290.

[94]. Hameren V.A. (2006). Goodness-of-fit tests in many dimensions. Nuclear Instruments, and Methods in Physics Research A, Vol. 559, p. 167 – 171.

[95]. D'Agostino, R. and Stephens, M. (1986). Mechanics of Particulate Matter-A Probabilistic Approach. New York: Marcel Dekker.

[96]. Bour, O. and Davy, P. (1997). Connectivity of random fault networks following a power law fault length distribution. Water Resour Res. 33 (7): 1567-1583.

[97]. Margolin, G., Berkowitz, B. and Scher, H. (1998). Structure, flow, and generalized conductivity scaling in fracture networks. Water Resour Res. 34 (9): 2103-2121.

[98]. de Dreuzy, J.R., Davy, P. and Bour, O. (2002). Hydraulic properties of two-dimensional random fracture networks following power-law distributions of length and aperture. Water Resour Res, 38(12), 1276, doi:10.1029/2001WR001009.

[99]. Wyllie, D.C. (1999). Foundations on Rock (2nd ed.). London, UK: Taylor and Francis.

[100]. Sharifzadeh, M., Mitani, Y., Esaki, T., & Urakawa, F. (2004). An investigation of joint aperture distribution using precise surface asperities measurement and GIS data processing. In K. Ohnishi

and Aoki (Ed.), 3rd Int Asian Rock Mech Symp, (pp. 165-171).

[101]. Bonnet, E., Bour, O., Odling, N.E., Davy, P., Main, I., Cowie, P. and Berkowitz, B. (2001). Scaling of fracture systems in geological media. Rev Geophys. 39 (3): 347–383.

[102]. Barton, N.R. (1973). Review of a new shear strength criterion for rock joints. Engineering Geology, 7, 287–322.

[103]. Warburton, P.M. (1980b). Stereological Interpretation of Joint Trace Data: Influence of Joint Shape and Implications for Geological Surveys. International Journal of Rock Mechanics and Mining Sciences, 17, 305-316.

[104]. Baecher, G., Lanney, N. and Einstein, H. (1977a). Trace length bias in joint surveys. 20th U.S. National Symposium on rock mechanics. Tahoe, Nevada.

[105]. Hakami, E., Einstein, H.H., Gentier, S. and Iwano, M. (1995). Characterization of fracture apertures - Methods and parameters. 8th Int Cong Rock Mech, (pp. 751-754). Tokyo.

تعیین توابع توزیع احتمال ویژگی‌های هندسی درزه‌ها

جمال زاده و عباس مجدی*

بخش مهندسی معدن، دانشگاه تهران، تهران، ایران

ارسال ۲۰۲۲/۰۳/۲۴، پذیرش ۲۰۲۲/۰۴/۱۱

* نویسنده مسئول مکاتبات: amajdi@ut.ac.ir

چکیده:

مکانیسم تغییر شکل و شکست سازه‌ها در داخل و روی توده‌سنگ‌های درزه‌دار اغلب توسط ویژگی‌های هندسی درزه‌ها کنترل می‌شود. از آنجایی که ویژگی‌های هندسی درزه‌ها طیفی از مقادیر دارند، درک توزیع این مقادیر به منظور پیش‌بینی چگونگی مقایسه مقادیر زیاد با مقادیر به‌دست‌آمده از یک نمونه کوچک مفید است. این کار سه مجموعه داده از سیستم درزه‌ها (۱۶۵۲ داده درزه‌ها) را از ۹ رخنمون سنگ‌های آذرین، رسوبی و دگرگونی به منظور تعیین تابع توزیع احتمال خواص هندسی درزه‌ها مورد مطالعه قرار می‌دهد. در نتیجه، آزمون‌های بهترین برازش (GOF) بر روی داده‌های به دست آمده اعمال می شود. طبق این آزمون‌ها، لاگ نرمال بهترین تابع توزیع احتمال است که فاصله‌داری، بازشدگی و طول درزه‌ها را نشان می‌دهد. کوشی بهترین تابع توزیع احتمال برای زاویه شیب درزه‌ها است. مشخص شد که تابع توزیع کوشی بهترین تابع توزیع احتمال برای نشان دادن جهت شیب درزه سنگ‌های آذرین است و تابع توزیع بور بهترین تابع توزیع احتمال برای تعریف جهت شیب درزه سنگ‌های رسوبی و دگرگونی است.

کلمات کلیدی: ویژگی‌های هندسی درزه‌ها، فاصله‌داری، بازشدگی، طول، آزمون‌های بهترین برازش.